Archaean andesite petrogenesis: insights from the Grædefjord Supracrustal Belt, southern West Greenland

Kristoffer Szilas [a, *], J. Elis Hoffmann [b, c], Anders Scherstén [d], Thomas F. Kokfelt [e], Carsten Münker [b]

[a] Lamont-Doherty Earth Observatory, PO Box 1000, Palisades, NY 10964-8000, USA

[b] Institut für Geologie und Mineralogie, Universität zu Köln, Zülpicher Str. 49b, 50674 Köln, Germany

[c] Steinmann-Institute, Universität Bonn, Poppelsdorfer Schloss, 53115 Bonn

[d] Department of Geology, Lund University, Sölvegatan 12, 223 62 Lund, Sweden

[e] Geological Survey of Denmark and Greenland - GEUS, Øster Voldgade 10, 1350 Copenhagen K, Denmark

ABSTRACT

We present new whole-rock major, trace and platinum-group element data, as well as Sm-Nd and Lu-Hf isotope data for meta-volcanic rocks from the Mesoarchaean Grædefjord Supracrustal Belt (GSB), located within the Tasiusarsuaq terrane, southern West Greenland. We also present new in-situ zircon U-Pb isotope data (by LA-ICP-MS) for associated felsic rocks. This region has experienced amphibolite to lower granulite facies metamorphism, causing re-equilibration of most mineral phases (including zircon).

An intrusive tonalite sheet with a zircon U-Pb age of 2888 ±6.8 Ma, yields a minimum age for the GSB. The Sm-Nd and Lu-Hf isotope data do not provide meaningful isochron ages, but the isotope compositions of the mafic rocks are consistent with the ca. 2970 Ma regional volcanic event, which is documented in previous studies of the Tasiusarsuaq terrane. The major and trace element data suggest a significant crustal contribution in the petrogenesis of andesitic volcanic

rocks in the GSB. The trace element variation of these andesitic leucoamphibolites cannot be explained by bulk assimilation-fractional-crystallisation (AFC) processes involving local basement. Rather, the observed patterns require binary mixing between basaltic and felsic end-member magmas with between 50-80% contributions from the latter (depending on the assumed felsic composition). Hf-isotope constraints point to contamination with pre-existing continental crust with an age of ca. 3250 Ma. Basement gneisses of this age were previously described at two localities in the Tasiusarsuaq terrane, which supports the mixing hypothesis. Thus the felsic end-member likely represents melts derived from the local basement.

Ultramafic rocks (18.35-22.80 wt.% MgO) in GSB have platinum-group element (PGE) patterns that are similar to magmas derived from high-degree melting of mantle, but they have relatively enriched trace element patterns. We propose that the ultramafic rocks represent arc-related picrites or alternatively were derived by melting of metasomatised sub-continental lithospheric mantle.

Overall these new geochemical data from the Mesoarchaean Grædefjord Supracrustal Belt and the petrogenetic mixing model in particular, are similar to observations from modern continental subduction zone environments, which also require large degrees of mixing with felsic basement melts. Therefore, we propose that the metavolcanic rocks formed in a modern-style subduction zone geodynamic setting, which due to the hotter Archaean mantle conditions allowed for substantial amounts of partial melting and magma mixing, rather than assimilating pre-existing continental crust.

Keywords: Archaean; Greenland; Grædefjord; Supracrustal belt; Andesite; Geochemistry

* Corresponding author.

E-mail address: kszilas@ldeo.columbia.edu (K. Szilas).

1. Introduction

Volcanic rocks of calc-alkaline andesitic composition are often regarded as a feature mainly associated with subduction zones (e.g. Kelemen et al., 2003). Here we present geochemical data for an assemblage of andesites of Mesoarchaean age from southern West Greenland. However, controversy exists about what type of geodynamic setting(s) operated during the Archaean and it is questioned by some if modern-style subduction zones even existed then (e.g. Bédard, 2006; Gerya, 2012; Van Kranendonk, 2011). Thus, it is relevant to study Archaean examples of andesites and evaluate their petrogenesis, because this may provide important constraints on the possible geodynamic setting that existed during the Archaean Eon.

The Archaean craton of Greenland has generally been interpreted in terms of a subduction zone model (e.g. Nutman and Friend, 2007; Polat et al., 2002; Windley and Garde, 2009), which is supported by the arc-like geochemistry of supracrustal rocks (Garde, 2007; Polat et al., 2011a; Szilas et al., 2012a, 2013), and the presence of hydrous primary magmatic minerals (Polat et al., 2012).

The Grædefjord supracrustal rocks presented in this paper represent yet another example of an Archaean supracrustal belt in southern West Greenland, which contains abundant andesitic rocks. The area surrounding Grædefjord was mapped during the Geological Survey of Greenland (GGU) mapping campaigns in southern West Greenland in the late 1960's. Later work on the Grædefjord Supracrustal Belt involved a M.Sc. thesis at the University of Copenhagen by Celina I.Z. Wilf (1982), focussing on the volcanogenic nature of the belt.

Polat et al. (2008) described Mesoarchaean andesitic rocks from the Ivisaartoq belt and Garde (2007) presented similar, but even more abundant, andesites from the Qussuk supracrustal belt, both located in the Nuuk region of southern West Greenland and both interpreted as having arc-related

origins. Similarly, Szilas et al. (2012a) ascribed the Mesoarchaean mafic to andesitic Ikkattup Nunaa Supracrustal Association south of the Fiskenæsset Complex to an arc-related geodynamic setting. In particular these andesites showed geochemical evidence of having an origin related to modern-style arc-processes, such as melting-assimilation-storage-homogenisation (MASH) by incorporating TTG-like felsic melts either in a magma chamber process or by melt-metasomatism of the mantle source of the andesites (Szilas et al., 2012a). Preliminary detailed geochemical studies of a relatively well-preserved volcanic section in the Kvanefjord region further support evidence for widespread occurrence of Mesoarchaean andesitic volcanic rocks in SW Greenland (Klausen et al., 2011). The relative abundance of metavolcanic rocks of intermediate compostion shows, that at least half of the supracrustal sequences, so far described in detail in southern West Greenland contain andesites *sensu stricto* with arc-like geochemistry (Garde, 2007; Klausen et al., 2011; Polat et al., 2007; Szilas et al., 2012a; this study). Thus, andesites are apparently more common in the North Atlantic craton than in Archaean cratons elsewhere in the world and therefore systematic studies of these andesites could help constrain the geodynamic processes that operated during the Mesoarchaean in this region.

2. Regional geology

The west Greenland part of the North Atlantic Craton consists of several Eo- to Mesoarchaean terranes ranging in age from ca. 3900 to 2800 Ma (e.g., Friend et al., 1988; Nutman et al., 1996; Nutman et al., 2007; Windley and Garde, 2009). The predominant rock type making up the different terranes are felsic gneisses of the tonalite-trondhjemite-granodiorite (TTG) suite. Scattered within the TTG domains are partly fragmented mafic supracrustal belts consisting predominantly of meta-basaltic rocks (now amphibolites) that were metamorphosed at amphibolite to lower granulite facies

conditions. Arguably some regions experienced granulite facies conditions, but were retrogressed to amphibolite facies metamorphic assemblages (e.g. Friend and Nutman, 2007; Riciputi et al., 1990; Schumacher, 2011). Late magmatic activity in the area is expressed by cross-cutting granite sheets.

The Grædefjord Supracrustal Belt is situated on the southern side of Grædefjord in the northern part of the Fiskenæsset region within the Tasiusarsuaq terrane (**Fig. 1**). This terrane is an extensive crustal block dominated by tonalite-trondhjemite-granodiorite (TTG) orthogneisses of mainly Mesoarchaean age and forms part of the North Atlantic craton (Kolb et al., 2012; Nutman et al., 1989). Early studies of the Fiskenæsset region concluded from field evidence that the supracrustal belts generally predate the regional TTG gneisses based on intrusive relationships (Kalsbeek and Myers, 1973). Geochronological work showed that the TTG gneisses yield ages of ca. 2880-2950 Ma (Kalsbeek and Pidgeon, 1980; Pidgeon and Kalsbeek, 1978), in good agreement with recent work based on Sm-Nd and Lu-Hf isochron ages on amphibolites and anorthosites of about 2970 Ma (Polat et al., 2010; Szilas et al., 2012a) and TTG gneiss ages of ca. 2900 Ma (Friend and Nutman, 2001; Kolb et al., 2012; Næraa and Scherstén, 2008; Szilas et al., 2012a). However, small fragments of older orthogneiss inclusions with ages of ca. 3250 Ma have also been described in the Tasiusarsuaq terrane (Næraa et al., 2012), which suggest that continental crust that predates the volcanic rocks did once exist in this region. The Ilivertalik granite is located immediately north-east of the Grædefjord Supracrustal Belt on the northern side of Grædefjord. It is charnokitic and commonly contains granulite facies mafic lenses with orthopyroxene and garnet. This granite represents a syn-tectonic intrusion with an age of 2795 +11/-7 Ma (Pidgeon and Kalsbeek, 1978).

The region is dominated by amphibolite facies rocks, although some show evidence for retrogression from granulite facies conditions in the form of orthopyroxene pseudomorphs within the orthogneisses (Chadwick and Coe, 1983; McGregor and Friend, 1992; Pidgeon and Kalsbeek,

1978). The first metamorphic event occurred around 2800-2700 Ma, with a second event following between 2670-2580 Ma (Crowley, 2002; Kolb et al., 2012). Peak metamorphic conditions in the Tasiusarsuaq terrane were estimated at 10.5 kbar and 810°C in mafic granulites and were followed by amphibolite facies retrogression at 7 kbar and 630°C (Riciputi et al., 1990). The retrogression was dated at ca. 2740-2700 Ma by U-Pb data from zircon, monazite and titanite (Crowley, 2002), consistent with the age of metamorphic zircon rims (Næraa and Scherstén, 2008; this study).

The Tasiusarsuaq terrane generally display an open to close fold pattern with southeast to south trending axial traces, however the area around the Grædefjord Supracrustal Belt is characterised by intense E-W trending cataclastic deformation and brittle-ductile mylonites (Kolb et al., 2010). The general high degree of deformation makes interpretation of primary magmatic features difficult. Nevertheless, Wilf (1982) described the presence of agglomerates, tuff beds and volcanic breccias in the leucoamphibolites of the Grædefjord Supracrustal Belt and interpreted this as a metamorphosed pyroclastic sequence.

3. Samples and petrography

The samples collected from the Grædefjord Supracrustal Belt (GSB) have been classified according to their field characteristics into the following petrographic groups: amphibolite, leucoamphibolite, mafic dyke, ultramafic rock, TTG gneiss and pegmatite. The samples used in this study were collected during field work lead by the Geological Survey of Denmark and Greenland (GEUS) in 2009.

The GSB comprises abundant leucoamphibolites of andesitic composition. We estimate that between 40-50% of the rocks in GSB are of this type of leucoamphibolite, and we admit that the present sample collection is moderately biased by an interest in this particular rock type. The

147 leucoamphibolites appear to be present only at the central part of the GSB, whereas dark
148 homogeneous amphibolite is exposed along the margin of the belt.

149 In the following we briefly described the main petrographic features of the different lithological
150 units:

151 The amphibolites are dark, medium-grained, hornblende-plagioclase-quartz-bearing rocks. They
152 are homogeneous and no primary structures are preserved. The foliation is defined by a hornblende
153 fabric. Mafic dykes are found in the northern part of the belt and are characterised by being
154 distinctly plagioclase-phyric (**Fig. 2a**). Angular multi-domained plagioclase phenocrysts (ocelli?) a
155 few centimetres in size are common in this lithological unit. The contacts to the mafic matrix
156 appears sharp in hand samples, but under the microscope irregular gradation of the plagioclase
157 contents is observed, which is perhaps related to metamorphic recrystallisation. Oxides generally
158 comprise less than 3 vol.% in the amphibolites.

159 The leucoamphibolites are grey, fine- to medium-grained, plagioclase-quartz-hornblende-biotite-
160 bearing rocks. Plagioclase often has a 'dirty' altered appearance from sericitisation. Biotite (up to
161 30 vol.%) and hornblende are oriented to give the rock a foliation, and modal variation often results
162 in banding from mm- to cm-scale (**Fig. 2c**). Quartz veins (mm- to cm-scale) are common in these
163 rocks. The leucoamphibolites often preserve various structures, such as fine grained modal layering
164 and fragments of various sizes, which have been interpreted to represent primary volcaniclastic
165 features (Wilf, 1982). Although breccias and agglomerates as described by Wilf (1982) were not
166 observed during the field work in 2009, well-preserved ash layers and possible volcanoclastic
167 bombs were found in low strain domains near the centre of the belt. The foliation bends around the
168 bomb-like inclusions and lithic fragments, as well as around locally observed diopside- and
169 hornblende porphyroblasts (**Fig. 2b**). The leucoamphibolites also preserve compositional layers
170 with modal variation of plagioclase and amphibole, which resembles volcaniclastic tuffs or ash flow

deposits (**Fig. 2c**) and possible volcaniclastic fragments (**Fig. 2d**). The contacts between the leucoamphibolites and the above-mention regular dark amphibolites are concordant and generally sharp, although a gradual transition is also observed in places. This suggests a volcanic depositional, rather than intrusive relationship between the two units.

Ultramafic rocks are generally rare, but have been found in one outcrop in the southern part of the belt. These rocks are fine grained, serpentine- and biotite-rich with less amphibole and epidote. They commonly contain calcite patches about 2-3 cm in size. They all contain about 10 vol.% oxides. One sample has large (mm-size) olivine grains. It is not clear from the field observations if this unit represents a discordant dyke or a co-genetic lava bed, due to structural transposition.

TTG gneisses are found throughout the Grædefjord Supracrustal Belt as discordant aplite sheets, as well as surrounding the belt with distinctly intrusive relationships along their contact. The TTG aplites are fine- to medium-grained, quartz-plagioclase-biotite-bearing and are mostly with a well-developed foliation. At one locality an intrusive gneiss band (ca. 3 m thick) contains plagioclase phenocrysts (<2 cm), which contain cores of magnetite rimmed by a fine grained dark green mineral.

Granitic pegmatites are observed to cut all rock types, although they are not abundant. They are medium- to coarse grained, quartz-alkali feldspar-plagioclase-biotite rocks. Feldspars are commonly dirty/altered in thin section.

4. Methods

Whole-rock major (by XRF) and trace element (by ICP-MS) data were acquired at the commercial ACME labs in Vancouver, Canada. Key samples were analysed for their ^{147}Sm-^{143}Nd and ^{176}Lu-^{176}Hf isotope compositions by MC-ICP-MS at the joint laboratories of Cologne and Bonn

195 universities. Radiometric age data consisting of U-Pb isotope compositions in zircon from intrusive
196 aplite sheets were measured at the Geological Survey of Denmark and Greenland (GEUS). Platinum
197 group elements (PGE) were measured on the three ultramafic samples at Université du Québec à
198 Chicoutimi following the procedure described by Savard et al. (2010). Detailed descriptions of the
199 analytical procedures can be found in **Appendix A** of the online supplementary material. All data
200 are available in **Tables 1-4** in the online supplementary material.
201
202 **5. Results**
203
204 5.1. Major, trace element and platinum group element geochemistry
205
206 The whole-rock major and trace element data are presented in **Table 1** and platinum-group
207 element (PGE) data for the three ultramafic samples are listed in **Table 2** in the online
208 supplementary material. In addition to analysis of PGEs in three samples from the Grædefjord
209 Supracrustal Belt (GSB), three samples from the Ikkattup Nunaa Supracrustal Association (Szilas et
210 al., 2012a) were also analysed for comparison. Below we briefly outline the main geochemical
211 features of the different lithological units. Supplementary geochemical diagrams can be found in the
212 online **Appendix B** and references to these are given the prefix 'B'.
213 Amphibolites (n = 4) have SiO_2 of 46.53-52.02 wt.%, TiO_2 of 0.60-1.19 wt.% and MgO of 4.95-
214 10.36 wt.% (**Fig. 3**). They are of tholeiitic basalt composition (**Figs. B1-B5**). Trace element range
215 as follows: 34.4-69.6 ppm Zr, 1.4-2.8 ppm Nb, 14.1-29.2 ppm Y, 17.4-75.0 ppm Ni and 27.4-280.5
216 ppm Cr (**Fig. 4**). The chondrite-normalised REE patterns are mostly flat with a La_{CN}/Sm_{CN} of 0.84-
217 1.25, La_{CN}/Yb_{CN} of 0.90-1.28 and Eu/Eu* of 0.88-0.98 (**Fig. B6**). Their primitive-normalised
218 patterns are generally flat, but have negative Nb-anomalies (calculated as Nb/Nb* =

$Nb_N/(\sqrt{(Th_N x La_N)})$ with Nb/Nb* of 0.59-1.08 (**Fig. 5**). The amphibolites in the GSB have flat trace element patterns that are similar to Archaean tholeiitic metabasalts found in other parts of the North Atlantic craton (e.g. Polat et al., 2008; Hoffmann et al., 2012; Szilas et al., 2013). They have subtle negative Nb-Ta anomalies and all but one sample (508219) plot above the mantle array in the Th/Yb vs. Nb/Yb Pearce diagram (**Fig. 6**).

Leucoamphibolites (n = 31) have a wide range of SiO_2 of 52.74-68.34 wt.% and MgO of 1.85-11.09 wt.%, and less so for TiO_2 of 0.39-0.86 wt.%. They straddle the border between being metaluminous and peraluminous (**Fig. B7**). The leucoamphibolites are of calc-alkaline affinity and have mostly andesitic compositions, although basaltic andesites and dacites also occur (**Figs. B1-B5**). Trace element concentrations range as follows: 78.1-221.3 ppm Zr, 3.4-7.9 ppm Nb, 8.5-18.0 ppm Y, 4.5-145.8 ppm Ni and 13.7-875.8 ppm Cr. The chondrite-normalised REE patterns are mostly steep with La_{CN}/Sm_{CN} of 2.71-5.74, La_{CN}/Yb_{CN} of 5.40-23.10 and Eu/Eu* of 0.69-1.12 (**Fig. B8**). Their primitive mantle-normalised patterns are moderately enriched, with negative anomalies for Nb (Nb/Nb* of 0.01-0.45), Ta and Ti, and variably negative anomalies for Sr and Pb (**Fig. 5**).

Mafic dykes (n = 3) have SiO_2 of 50.19-52.02 wt.%, TiO_2 of 0.83-0.96 wt.% and MgO of 4.03-6.19 wt.%. They are generally of tholeiitic basaltic composition (**Figs. B1-B5**). Trace element range as follows: 49.3-62.1 ppm Zr, 2.4-2.7 ppm Nb, 19.6-23.2 ppm Y, 11.5-32.6 ppm Ni and 82.1-205.3 ppm Cr. The chondrite mantle-normalised REE patterns are mostly flat with a La_{CN}/Sm_{CN} of 1.37-2.17, La_{CN}/Yb_{CN} of 1.47-2.29 and Eu/Eu* of 0.90-0.95 (**Fig. B9**). Their primitive mantle-normalised patterns are generally flat, but have negative Nb-anomalies with Nb/Nb* of 0.19-0.40 (**Fig. 5**). The mafic dykes are geochemically similar to the amphibolites in many ways, but they are characterized by elevated Th, U and LREE concentrations relative to the amphibolites. This results in more pronounced negative Nb-Ta anomalies and they fall well within the arc-field of the Th/Yb vs. Nb/Yb Pearce diagram (**Fig. 6**).

Ultramafic rocks (n = 3) have SiO_2 of 45.78-51.87 wt.%, MgO of 18.35-22.80 wt.% and TiO_2 of 1.00-1.25 wt.%. Trace element range as follows: 56.8-70.5 ppm Zr, 10.6-14.2 ppm Nb, 10.3-13.5 ppm Y, 337.0-601.2 ppm Ni and 1388.9.-1724.2 ppm Cr. The chondrite-normalised REE concentrations show fairly enriched patterns with La_{CN}/Sm_{CN} of 1.68-2.22, La_{CN}/Yb_{CN} of 5.99-8.19 and with variable negative Eu anomalies (Eu/Eu* of 0.69-0.90) (**Fig. B10**). Their primitive mantle-normalised patterns are moderately enriched, with positive anomalies for Nb (Nb/Nb* of 1.16-1.82) and Ta, and strong negative anomalies for Pb and Sr (**Fig. 7**). The chondrite-normalised (Fisher-Gödde et al., 2010) PGE patterns show fractionated positive slopes with smoothly increasing trends from Os to Pd (**Fig. 8**).

TTG gneisses (n = 5) have SiO_2 of 69.97-76.38 wt.%, TiO_2 of 0.07-0.23 wt.% and MgO of 0.24-0.51 wt.% and are of calc-alkaline affinity. Trace element range as follows: 67.5-251.1 ppm Zr, 3.5-8.9 ppm Nb, 5.3-28.3 ppm Y, 0.1-3.5 ppm Ni and <13.7 ppm Cr. The chondrite-normalised REE concentrations show fairly enriched patterns steep with La_{CN}/Sm_{CN} of 4.65-6.42, La_{CN}/Yb_{CN} of 10.30-113.84 and with variably negative Eu anomalies (Eu/Eu* of 0.60-0.90) (**Fig. B11**). Their primitive mantle-normalised trace element patterns are strongly enriched, and they have negative anomalies for Nb (Nb/Nb* of 0.03-0.17), Ta, Pb, Sr and Ti (**Fig. 5**).

5.2. Sm-Nd and Lu-Hf isotope compositions

Eight whole-rock samples were analysed for their Sm-Nd and Lu-Hf isotope compositions using isotope dilution techniques and measurement by MC-ICP-MS at the joint laboratories of Cologne/Bonn at the Steinmann-Institute (see method details in **Appendix A**). The Sm-Nd and Lu-Hf isotope results are presented in **Table 3** in the online supplementary material.

We have calculated the initial εNd_t and εHf_t using the minimum age constraint of 2888 Ma from a crosscutting TTG sheet (see **Section 5.3**) and at 2970 Ma, which is the age of the nearby Fiskenæsset Anorthosite Complex (Polat et al., 2010) and the Ikkattup Nunaa Supracrustal Association (Szilas et al., 2012a). Nevertheless, we have also calculated initial εNd_t and εHf_t at 3200 Ma to see what their hypothetical isotope compositions would be at this time, although this age seems unlikely for the GSB.

Unfortunately, none of the two isotopic systems provide meaningful isochron ages for the rocks of the Grædefjord Supracrustal Belt (GSB). The reason for this is that either these rocks are not co-genetic, or they were derived from different mantle sources or else this simply means that some of them have been disturbed by crustal contamination.

The Sm-Nd system yields an isochron age of about 3300 Ma for all samples, whereas the Lu-Hf system yields an isochron age of about 3200 Ma. These ages are similar to their DM-model-ages, but the large errors (>100 Ma) and high mean standard weighted deviations (MSWD >40), suggest an influence of metamorphic disturbance, crustal contamination or dissimilar mantle sources.

The reader is referred to the online supplementary **Table 3** for the ranges of the calculated ε-values at the three different ages. **Figure 9** shows the εHf_t evolution of the samples since 2970 Ma and the εNd_t evolution is presented in **Appendix B** (**Fig. B12**). It is worth noting that εHf_{2970Ma} and εNd_{2970Ma} correlate positively with 1/Hf and 1/Nd, respectively (**Figs. B13 and B14**) and the same is the case when these initial ε-values are plotted against Th/Yb and Nb/Nb*.

5.3. In-situ zircon U-Pb isotope data

Zircon separated from two TTG gneisses, one granitic pegmatite, three leucoamphibolites and one mafic dyke were analysed for their U–Pb isotope compositions by LA-ICP-MS at the

290 Geological Survey of Denmark and Greenland (see method details in **Appendix A**). Spots were
291 mainly aimed at igneous zircon cores to obtain intrusion ages, although some metamorphic rims
292 were also included in the analysis. The U–Pb isotope data are presented in **Table 4** in the online
293 supplementary material. Concordia diagrams and probability density diagrams (PDD) were plotted
294 using the Isoplot software for Excel (Ludwig, 2003) and are presented in **Appendix B** of the online
295 supplementary material. All of these rocks show strong metamorphic disturbance by the ca. 2720
296 Ma regional event (Crowley, 2002; Næraa and Scherstén, 2008). Therefore we have resorted to use
297 unmixing models to filter out scatter and older tails in the concordia diagrams.

298 TTG sample 511110 was measured in two sessions, but the data were pooled to yield more
299 robust statistics. The PDD in **Fig. B15a** shows a peak close to 2900 Ma that is skewed slightly
300 towards lower ages. A two-component unmixing model shows a peak at ca. 2898 and 2834 Ma.
301 When the data is filtered for the younger component a concordia plot yields a regression line with
302 an age of 2888.0 ±6.8 Ma (**Fig. B15b**).

303 TTG sample 508221 shows a normal distribution with one outlier at ca. 2803 Ma, which may
304 represent an inherited grain (**Fig. B15c**). When the outlier is removed from the data the regression
305 line in the concordia diagram yields an age of 2708 ±11 Ma (**Fig. B15d**).

306 Pegmatite sample 511134 shows one dominant peak at ca. 2700 Ma and one sub-peak at ca.
307 2800 Ma (**Fig. B15e**). When filtering the data for the sub-peak the regression line in the concordia
308 diagram yields an age of 2731 ±19 Ma (**Fig. B15f**).

309 **(INSET INLINE FIGURE B15 HERE)**

310 Leucoamphibolite sample 508223 has a main peak around 2728 Ma, but is skewed slightly
311 towards older ages (**Fig. B16a**). A two component unmixing model reveals a possible component at
312 around 2772 Ma. When the latter is removed from the data the regression line in the concordia
313 diagram yields an age of 2729.6 ±8.2 Ma (**Fig. B16b**).

Leucoamphibolite sample 508227 shows a normal distribution in the PDD (**Fig. B16c**), and the regression line in the concordia diagram yields an age of 2713.9 ±9.2 Ma (**Fig. B16d**).

Leucoamphibolite sample 511142 has a main peak around 2720 Ma, but is skewed towards older ages (**Fig. B16e**). A three component unmixing model reveals a possible component at around 2775 Ma. When data older than the latter are filtered out, the regression line in the concordia diagram yields an age of 2721 ±13 Ma (**Fig. B16f**).Mafic dyke sample 508218 shows a normal distribution except for one outlier at ca. 2824 Ma (**Fig. B17a**). When this outlier is removed from the data the regression line in the concordia diagram yields an age of 2717.5 ±7.6 Ma (**Fig. B17b**).

(INSET INLINE FIGURE B16 HERE)

(INSET INLINE FIGURE B17 HERE)

6. Discussion

6.1. Assessment of major and trace element mobility

An influence of element mobility on the major and trace element compositions, as a result from post-magmatic alteration, has been described previously from several supracrustal belts in southern West Greenland (e.g., Polat and Hofmann, 2003; Rose et al., 1996; Szilas et al., 2012a, Szilas and Garde; in press). The rocks of the Grædefjord Supracrustal Belt (GSB) were deformed to various degrees and were metamorphosed to amphibolite and lower granulite facies (Kolb et al., 2010, 2012). Therefore it is a possibility that fluid-mobile elements in particular could have been disturbed during post magmatic events.

However, following the weathering index of Ohta and Arai (2007) the samples fall on the igneous fractionation line, providing evidence that secondary processes had only minor influence on

the major element compositions (**Fig. B18**). Nevertheless, we rely only on the least mobile trace elements (HREE, HFSE and some transition metals) for the petrogenetic interpretations, as these have been shown to be largely unaffected by post-magmatic processes (e.g., Hoffmann et al., 2012; Polat and Hofmann, 2003; Polat et al., 2002, 2007; Szilas and Garde, in press). Although disturbance of these elements cannot be fully excluded, and some scatter is likely the result of mild alteration, weathering and/or metamorphic modification, the samples from the different lithological groups generally form coherent trends in variation diagrams (**Figs. 3-4**). The observed trends are consistent with those expected for the igneous processes that we discuss in the following sections.

6.2. Evaluation of fractional crystallisation, assimilation and magma mixing

The trace element and isotope compositions of igneous rocks can be influenced by various magmatic processes, such as fractional crystallisation, assimilation of older crustal components and binary magma mixing processes (e.g., DePaolo, 1981; Perugini and Poli, 2012). Hence, in the following section we evaluate the potential influence of such processes on the different rock types found in the GSB.

The amphibolites have variably depleted isotope compositions (**Fig. 9**; εHf_{2970Ma} +3.7 to +6.8 and **Fig. B12**; εNd_{2970Ma} +3.6 to +4.6). Their trace element patterns are parallel to each other resembling primary mantle melts. Therefore we consider it unlikely that assimilation or mixing processes influenced their isotope compositions. The Hf-Nd isotope heterogeneity is rather likely to reflect the tapping of variably depleted mantle sources. This interpretation is similar to what has been concluded for other basaltic rocks with tholeiitic trace element patterns from other Mesoarchaean supracrustal belts in southern West Greenland (Polat et al., 2008; Hoffmann et al., 2012; Szilas et al., 2013). Furthermore, there is direct evidence against a relationship between the

mafic and andesitic rocks resulting from fractional crystallisation (FC). Firstly, their trace element patterns are distinctly different with no intermediate patterns (**Fig. 5**) and secondly the andesites form fanned rather than linear arrays in variation diagrams (**Fig. 3 and 4**). The amphibolites and the mafic dykes form a sub-vertical trend in the Pearce diagram (**Fig. 6**), which could reflect a subduction zone component with recycling of older unradiogenic sediments or alternatively minor mixing with slab melts (Kessel et al., 2005; Klimm et al., 2008). Their isotope compositions do not suggest significant crustal contamination.

The calc-alkaline leucoamphibolites are mainly andesites with many similarities to modern arc rocks (e.g. enrichment in LREE, Th, U and negative Nb-Ta anomalies relative to MORB), however they do generally possess negative Pb and Sr anomalies, which are usually not seen in modern volcanic arc rocks (e.g. Kelemen et al., 2003). It remains a possibility that extensive regional metamorphism caused post-magmatic mobilisation of Pb and Sr, which could have been lost to a fluid phase, but we do not find correlation with other fluid mobile trace elements. It is important to note that similar supracrustal rocks from the INSA also share these unusual negative Pb and Sr anomalies, whereas anorthosites from the Fiskenæsset Complex are strongly enriched in these two trace elements (Polat et al., 2011b; Szilas et al., 2012a). This suggests that the extensive anorthosite bodies of the Fiskenæsset region are co-genetic with both the GSB and INSA supracrustal rocks and that Sr and Pb were fractionated by the segregation of the anorthosite. One possible interpretation would be that the supracrustal belts represent the surface expressions of an arc complex, whereas the Fiskenæsset Complex represents the middle to lower arc crust. Alternatively, the negative Pb and Sr anomalies are simply a general feature of the Archaean geodynamic setting in which these volcanic rocks formed.

In contrast to the mafic lithologies, the leucoamphibolites have rather low εNd_{2970Ma} and εHf_{2970Ma} of zero (**Fig. 9**), whereas the estimated depleted mantle value of εH_t at 2970 Ma is about

386 +6. Therefore, crustal contamination with older less radiogenic crust might have led to the observed
387 difference. By plotting the isotope data of the lithological units (amphibolites, dykes and
388 leucoamphibolite) into 1/Nd and 1/Hf diagrams a positive correlation with the initial εHf_{2970Ma} and
389 εNd_{2970Ma} values is observed (**Figs. B13-14**). This could indeed be explained by crustal
390 contamination or binary mixing. However, the fact that the leucoamphibolites do not form a
391 continuum, in terms of trace element abundances extending from the basaltic amphibolites toward
392 the TTGs, suggests that the contamination might not have been due to bulkassimilation fraction
393 crystallization (AFC) processes. This is interpretation is supported by their restricted range in
394 element variation diagrams (**Figs. 3-4**), their nearly constant trace element patterns (**Fig. 5**) and by
395 the tight clusters of εNd_{2970Ma} and εHf_{2970Ma} for each lithological unit (**Fig. 9**).
396 We have modelled the observed trace element variations of the meta-volcanic rocks by
397 calculating fractional crystallisation (FC), bulk assimilation and fractional-crystallisation (AFC), as
398 well as binary magma mixing trends using the Excel spread sheet program of Ersoy and Helvacı
399 (2010). For practical purposes we have used the median values of the five local TTG samples
400 presented in this study, as an approximation of the regional TTG crust that may have acted as a
401 contaminant. Although these TTGs are clearly younger than the supracrustal rocks, we justify this
402 approximation by the fact that the geochemical compositions of the TTGs are fairly homogeneous
403 throughout this region, regardless of their age (Kolb et al., 2012). However, we also did the
404 calculations with several different types of TTG as the contaminant and the younger TTG-type
405 analogue represented by the median Grædefjord TTG did in fact yield the most reasonable results,
406 because many other end-members had too low contents of incompatible trace elements.
407 The TTG gneisses have major and trace element compositions that fall within those of Archaean
408 TTGs and bear some resemblance to modern adakites (e.g. Martin, 1999; Martin and Moyen, 2002;
409 Martin et al., 2005). For certain major and trace elements the TTGs form an end-member, which

suggests mixing with basalts to produce the leucoamphibolites (**Figs. 3-4**). This mixing hypothesis is supported by the clear isotopic evidence for crustal contamination of the leucoamphibolites and also by our trace element modelling (**Figs. B19-B22**).

Fractional crystallisation is not able to cause evolution of the basaltic magmas to the andesitic magmas in this case, as seen by their distinctly different trace element patterns and the lack of transitional compositions (Fig. 5). Another important observation from our trace element modelling is that none of the trace element trends can be explained by a bulk assimilation-fractional-crystallisation (AFC) model, even if we assume an unrealistically high r-ratio of 0.9 (**Fig. 10**). In fact the modelling consistently point towards magma mixing to produce the observed trends (**B19-B22**). Therefore we find that a simple binary mixing model between the local Grædefjord TTGs and the amphibolites can explain the composition of the leucoamphibolites for most elements. This is also suggested by the variation diagrams, where the data for the leucoamphibolites fan out from the TTGs towards the mafic end-members (**Figs. 3-4**). However, there are a few exceptions, such as CaO, P_2O_5, Sr, Nb and Ta, which are all slightly elevated in the leucoamphibolites relative to the mixing arrays between various combinations of the TTGs and amphibolites. Thus the local TTGs are probably not a perfect proxy for the actual contaminant or perhaps the anomalous elements were supplied by an additional component, such as subducted sediments or slab-derived melts. Interestingly, Szilas et al. (2012a) also found that certain leucoamphibolites of the Ikkattup Nunaa Supracrustal Association (INSA) showed enrichment of the above mentioned elements, and argued for a low silica adakite component produced by slab melting to explain the data. In addition, Ni and Cr are also elevated in the leucoamphibolites and form vague trends towards the ultramafic rocks, indicating that perhaps ultramafic cumulates, picritic melts or mantle rocks were also involved in the petrogenesis of the leucoamphibolites.

The fact that our modelling requires mixing of 50-80% TTG-like melts with mafic material similar to the Grædefjord amphibolites (**Figs. 10 and B19-B22**), essentially rules out bulk AFC processes, because this would require far too great amounts of crystallisation to supply the heat for melting of the contaminant. Therefore we can reject the possibility of contamination during ascent of mafic magmas through pre-existing continental crust. However, the exact proportion of felsic end-member depends on the assumed TTG composition, but regardless of this, binary mixing is required to explain the observed trace element variation. On the other hand, the Sm-Nd and Lu-Hf isotope data also clearly necessitate some form of contamination/mixing with pre-existing unradiogenic crust with low initial εNd_t and εHf_t values. We discuss a possible geodynamic model for the mixing of mafic and felsic magmas in the petrogenesis of the andesitic leucoamphibolites in **Section 6.6**. We note that the mechanism of chaotic mixing could possibly explain some of the geochemical variation, which is observed in the leucoamphibolites by differential diffusion of elements during mixing between mafic and felsic end-members (e.g. De Campos et al., 2011; Morgavi et al., 2012; Perugini et al., 2012).

6.3. Geochemical characteristics of the ultramafic rocks

The ultramafic rocks from the Grædefjord Supracrustal Belt (GSB) are moderately enriched in incompatible trace elements and the negative slope of their HREE suggests presence of garnet in their source (**Fig. 7**). They also have the same unusual negative Sr- and Pb-anomalies, as the volcanic rocks of GSB. As previsouly mentioned in **Section 6.2**, the anorthosite bodies in the Fiskenæsset region, which are of similar age, have correspondingly positive Pb and Sr anomalies (Polat et al., 2010, 2011b). This suggests that the regional metavolcanic supracrustal belts (GSB and INSA) are co-genetic with the Fiskenæsset Complex as discussed above.

The Grædefjord ultramafic rocks have platinum-group element (PGE) patterns that resemble those of mantle-derived melts (**Fig. 8)**, which generally have positive fractionated PGE patterns and higher abundances with decreasing compatibility (e.g. Bézos et al., 2005). In addition we have analysed three samples from the Ikkattup Nunaa Supracrustal Association (INSA), which were interpreted to represent ultramafic cumulate rocks (Szilas et al., 2012a). The cumulates from INSA show complicated patterns with anomalies for Ru and Rh. This is consistent with variable sulfide and/or chromite contents in the cumulates, which cause different degrees of fractionation of the PGEs. The fact that the ultramafic rocks in Grædefjord have melt-like PGE patterns, which are similar to the median abundances of different types of komatiites (data from Fiorentini et al., 2011), suggest that they are not cumulates but represent magmas (**Fig. 8**).

Interestingly, two ultramafic samples with similar enriched trace element patterns, as observed for the GSB ultramafic rocks, were reported from a locality less than 100 km NE of Grædefjord by Kolb et al. (2012), suggesting a regional occurrence of such rocks. When taking into account that depleted ultramafic rocks of Ti-enriched komatiitic affinity occur on the nearby 'Nunatak 1390' (Szilas et al., 2012b), we find a striking resemblance to the reported association of enriched and depleted ultramafic rocks in a Palaeoproterozoic supracrustal belt in northern Finland (Hanski et al., 2001). Also noteworthy is the observation of picrites from Finland by Hanski and Kamenetsky (2013), which contain melt inclusion of both enriched and depleted ultramafic composition within single spinel grains. This suggests that these two compositionally distinct melts were genetically related. A similar association of enriched and depleted ultramafic rocks were also reported by Goldstein and Francis (2008) in an association of ferro-picrites from Archaean supracrustal belts in the Western Superior Province, Canada.

The subcontinental lithospheric mantle (SCLM) that underlies the North Atlantic craton in southern West Greenland (Wittig et al., 2008) has somewhat similar enriched trace element

patterns, with the exception that it generally has positive Sr and Pb anomalies. The similar enrichments of incompatible trace elements does suggest that the metasomatising agent that affected the SCLM could also be responsible for the enrichment found in the Grædefjord ultramafic rocks, perhaps by metasomatising their mantle source. Weiss et al. (2011) proposed that such metasomatism of the SCLM is caused by high-Mg carbonatitic high-density fluids and kimberlite melts. Accordinly, it is possible that the mantle source of the Grædefjord ultramafic rocks may also have interacted with similar exotic components causing their unusual trace element composition. Therefore, the Grædefjord ultramafic rocks may represent magmas derived by actual melting of the local SCLM.

Given the limited data on these ultramafic rocks, we can only speculate about the geodynamic setting in which these different possible processes could have occurred. However, we do note that the Grædefjord ultramafic rocks have trace element patterns that are similar modern picrites from the Lesser Antilles, including the negative Pb and Sr anomalies for some of the latter (Thirlwall et al., 1996). Thus, it appears even more likely that deep high-degree melting of garnet-lherzolite in a subduction zone environment was responsible for the unusual geochemical compositions of the GSB ultramafic rocks. This also appears compatible with a model in which anorthosite segregation was responsible for the regional negative Pb and Sr anomalies, which are observed in virtually all lithological units in GSB. In this model the GSB represents the shallow volcanic environment of an arc complex, whereas the Fiskenæsset Complex would represent the deeper intrusive and cumulate portion of this subduction zone system. However, at the moment the petrogenesis of the Grædefjord ultramafic rocks remains enigmatic and future studies are needed to resolve this question.

6.4. Sm-Nd and Lu-Hf isotope constraints

505 It is well-documented that the Sm-Nd isotope system is not as robust as the Lu-Hf isotope
506 system in most metamorphosed rock types, whereas the former can be disturbed during alteration
507 and metamorphism (e.g. Gruau et al., 1996; Hoffmann et al., 2011; Polat et al., 2003; Rosing, 1990;
508 Thompson et al., 2008). Therefore we emphasise the Lu-Hf over Sm-Nd systematics in the
509 discussion of the isotope data. However, this assumption requires that there is a mineral host for Lu
510 and Hf.

511 We note that even the Lu-Hf system yields very high MSWD (>40) for the isochron and errors
512 over 100 Ma. This is likely due to the fact that the samples have very different initial isotope
513 compositions at 2970 Ma, resulting from a combination of various processes including mixing,
514 source heterogeneity, inheritance of older crust and/or metamorphic disturbance, which rendered
515 the Lu-Hf and Sm-Nd isochron ages meaningless.

516 Given the great abundance of supracrustal and gabbro-anorthosite rocks in this region with an
517 age of ca. 2970 Ma (e.g. Hoffmann et al., 2012; Polat et al., 2010, Szilas et al., 2012a, 2012b) we
518 speculate that this is also the likely magmatic age for the Grædefjord Supracrustal Belt (GSB). This
519 is supported by the fact that four of five mafic samples from GSB fall on the isochron line presented
520 by Szilas et al. (2012a) as seen in **Fig. B23**.

521 **(INSET INLINE FIGURE B23 HERE)**

522 Additionally, the εHf_{2970Ma} of one amphibolite sample (511116) from GSB fall directly on the
523 DM-array at 2970 Ma. However, the rest of the amphibolites and mafic dykes have εHf_{2970Ma} at
524 around +4 and the leucoamphibolites have values around 0 (**Fig. 9**). Thus, these two groups appear
525 to have been influenced by crustal contamination by two distinct processes with limited isotope
526 ranges. It is also worth noting that the GSB data plots on the exact same three source regions (**Fig.**
527 **B24-B25**) as those found by Szilas et al. (2012a) for INSA. This further substantiates the great
528 resemblance of these two supracrustal sequences. Although impossible to prove with the current

data there is the remote possibility that the Tasiusarsuaq hosted crust with a chondritic Sm-Nd and Lu-Hf isotopic composition at 2970 Ma, as displayed in **Figs. B24-B25**. This is partly supported by the Hf isotope data of Souders et al. (2012), which also show a possible near-chondritic influence. However, this may simply be a coincidence.

An important fact is that rememnats of TTG crust have been documented from the Tasiusarsuaq terrane, which predates the likely igneous age of 2970 Ma for the GSB. One such example is TTG gneiss sample 515747 with a zircon age of 3260 Ma (T. Næraa, unpublished data) and also sample 468645 of Næraa et al., (2012). **Figure 11** shows the evolution of $^{176}Hf/^{177}Hf$ of the GSB rocks, as well as that of the 3255 Ma old TTG gneiss sample 468645 of Næraa et al. (2012). We have used the average data of four analyses older than 3200 Ma from sample 468645 to calculate the possible Hf-isotope evolution of pre-existing continental crust in the Tasiusarsuaq terrane. Mixing between this crust and juvenile mafic magma at 2970 Ma shows remarkably similar mixing ratios (ca. 60% TTG-like component), as what we obtained from our trace element modelling (ca. 50-80%). This further supports our model for the andesitic leucoamphibolites, as the product of mixing between mafic and felsic magmas in a ratio of about 2:3.

6.5. U-Pb zircon age constraints

The U-Pb isotope data point towards a significant event at ca. 2720 Ma, which affected the all of the Grædefjord supracrustal rocks. This is in good agreement with the regional metamorphic event identified in the Tasiusarsuaq terrane (Crowley, 2002; Kolb et al., 2012). Wilf (1982) obtained an age of 2709 ±30 Ma for a 19 point Rb-Sr isochron on the leucoamphibolites, which is in good agreement with the U-Pb zircon data presented in this paper (**Section 5.3**). The mobility of both Rb and Sr suggest that this age reflects metamorphic resetting rather than an igneous age. This

553 is consistent with the minimum age of 2888 ±6.8 Ma for the supracrustal rocks as dated by the
554 intrusive TTG gneiss (**Fig. B15a-b**). It is surprising that TTG sample 508221 points to an age of ca.
555 2700 Ma, but this indicates that the metamorphic event was associated with intrusion of TTG sheets
556 or perhaps that some were reset by this event. However, the same ages of metamorphic zircons and
557 magmatic zircons from TTGs have been observed for TTG samples from the Naajat Kuuat
558 Complex, which is also part of the Tasiusarsuaq terrane (Hoffmann et al., 2012). There, the 2800
559 Ma zircon age has been interpreted in previous studies to reflect the granulite facies metamorphic
560 event (Nutman and Friend, 2007), whereas the 2700 Ma event was interpreted to be associated with
561 the terrane accretion with the Tre Brødre terrane (e.g., Hoffmann et al., 2012).
562 We have no explanation for the abundant magnetite, rimmed by plagioclase that is found in some
563 of the TTG sheets, but we do note that abundant magnetite phenocrysts are also observed in modern
564 rhyolites associated with boninites in the Izu-Bonin arc (Woodland et al., 2002).
565 The pegmatite sample (511134) has a minor peak around 2800 Ma, and an adjacent much larger
566 peak at 2700 Ma, which we interpret is due to metamorphic thermal overprinting (**Fig. B15e-f**).
567 Thus its true magmatic age is probably around 2800 Ma. Alternatively, the true age is in fact 2700
568 Ma with a distinct inherited population. With the present data we are not able to distinguish
569 between these two possibilities.
570 All zircon ages in the leucoamphibolites represent the regional metamorphic event with virtually
571 no relict magmatic grains. Two of the leucoamphibolites show small tails towards older ages, which
572 we interpret to reflect intense metamorphic resetting of magmatic zircon that has essentially
573 obliterated any older grains. Evidence for this type of resetting of volcanic zircon was described in
574 similar leucoamphibolites from INSA (Szilas et al., 2012a).
575 The zircon age of ca. 2717 Ma the mafic dyke sample (508218) also likely reflects late
576 metamorphic zircon growth, because mafic rocks rarely carry magmatic zircon and because this

sample has initial εNd_t and εHf_t, which falls well within the range of the other measured Grædefjord rocks.

6.6. A model for Archaean andesite petrogenesis

Essentially every single supracrustal belt, that has been studied in detail, in southern West Greenland is comprised of mainly tholeiitic basalts with distinctly negative Nb- and Ta-anomalies (e.g. Garde, 2007; Polat et al., 2008; Szilas et al., 2012a, 2012b, 2013). Such mafic belts always predate the surrounding intrusive TTG orthogneisses, unless the contacts are tectonic as in the case of the Storø Supracrustal Belt (van Gool et al., 2007). However, as discussed in **Section 6.4** sporadic evidence suggests minor relicts of pre-existing crust also exists in the Tasiusarsuaq terrane (Næraa et al., 2012). The relatively great abundance of andesites that have been identified in the Archaean supracrustal belts of southern West Greenland in recent years (see **Section 1**), show that such rocks are likely more common in this region than in other cratons. Based on our field work, we estimate that in the Grædefjord Supracrustal Belt, andesites comprise about 40-50% of the exposed meta-volcanic rocks. However, the lack of firm field relationships between the different lithological units complicates this estimate and there is a large uncertainty as to how much of the primary volcanic sequence has actually been preserved.

The geochemical data of Szilas et al. (2012a) for andesites from the Ikkattup Nunaa Supracrustal Association (INSA) located about 100 km SE of the Grædefjord Supracrustal Belt (GSB), shows that the two basaltic to andesitic sequences bear great resemblance. Their trace element patterns are very similar, although there are minor differences in their absolute elemental abundances. Isotopically they are also quite similar with the exception that the leucoamphibolites of the GSB have distinctly lower (around 0) initial εNd_t and εHf_t (**Figs. B24-B25**). Based on geochemical

arguments, Szilas et al. (2012a) concluded that the rocks of INSA likely formed in a subduction zone geodynamic setting. Given the great similarity between INSA and GSB, it is tempting to assume the same geodynamic environment of formation for the latter. The striking geochemical resemblance between modern arc andesites and the GSB andesites does indeed support this assumption. Furthermore, Polat et al. (2011b) also concluded that the nearby Fiskenæsset Complex was formed by subduction zone processes. Thus there seems to be growing evidence of a significant magmatic event at ca. 2970 Ma in the Tasiusarsuaq Terrane, which was associated with subduction zone volcanism.

We need to point out an important correction to the work of Szilas et al. (2012a); because they concluded that the leucoamphibolites of INSA are juvenile.We find that these rocks do in fact plot below the depleted mantle (DM) array at between +3.6 to +5.2, when using the DM-evolution line of Griffin et al. (2000) for the Lu-Hf isotope system. However, the INSA volcanic rocks do not have as low isotopic compositions ($\varepsilon Hf_{2970Ma} = 0$) as the most enriched rocks from GSB. The INSA data does also not show the same good correlations between initial εNd_t vs. 1/Nd, Th/Yb, Nb/Nb* and εHf_t vs. 1/Hf, Th/Yb, Nb/Nb* that the data from the GSB shows (**Figs. B13-B14**). The revision regarding the juvenile composition of the INSA has important implications for the conclusions of Szilas et al. (2012a), and we find that the model presented below for the GSB is probably more appropriate also for the INSA considering the strong geochemical resemblance of these two supracrustal sequences.

Any geodynamic model for the GSB must take the obvious mixing relationships seen in the leucoamphibolites into account (**Section 6.2**). Given that we can rule out bulk AFC-processes (**Figs. 10 and B19-B22**), the extensive degrees of mixing between TTG-like magmas and juvenile mafic magmas must have occurred in a well-mixed magma chamber. It also seems likely that this mixing could have occurred slightly before or after the eruption of the mafic magmas. This would explain

625 the observation that we do not find a geochemical gradation between the mafic and andesitic rocks,
626 neither in terms of major or trace elements, nor in terms of their isotopic compositions. It is possible
627 that the mafic sequence represents an early juvenile stage of volcanism, but it also remains possible
628 that they erupted after the andesites, once a stable conduit had formed and crustal mixing was no
629 longer occurring. However, we cannot resolve this temporal issue with the present isotope data and
630 the field relationships do also not provide evidence for wither case.

631 Several lines of evidence point to an active continental margin setting in which mafic magmas
632 interacted with pre-existing crust. This is suggested by the TTG-type mixing end-member and the
633 resulting binary major and trace element trends, as well as by the distinctly unradiogenic
634 contaminant (Fig. 11). A subduction zone setting would accommodate the general picture that has
635 emerged for southern West Greenland based on previous geochemical (Polat et al., 2011a; Szilas et
636 al., 2012a) and structural studies (Kisters et al., 2012; Kolb et al., 2012). We note that the
637 Grædefjord andesites are virtually identical to andesites and dacites from the ca. 2724 Ma Lac
638 Lintelle sequence in the Vizien greenstone belt (Skulski and Percival, 1996) and andesites from the
639 ca. 2800-2680 Ma Schreiber–Hemlo greenstone belt (Polat et al., 1998), Superior Province, Canada.
640 These andesitic rocks were interpreted to have formed in a continental arc volcanic complex. There
641 are also some resemblance to 2700 Ma andesites of the Wawa greenstone belt, Superior Province
642 (Polat and Kerrich, 2001).

643 According to the Georoc database (2013), the major and trace element geochemical
644 compositions of the mafic to andestic volcanism recorded by GSB, are comparable to the
645 compositions of andesites that are sampled in modern mature island arcs (except for the unusual
646 negative Pb and Sr anomalies in all samples of the GSB).

647 A sanukitoid-type origin for the GSB andesites can be excluded due to the different geochemical
648 compositions and modes of occurrence. Sanukitoids are granitoid rocks that are characterised by a

high content of incompatible trace elements in combination with a high content of compatible trace elements, such as MgO, Cr and Ni (Stern et al., 1989). They are generally interpreted as melts derived from a crustally contaminated mantle source, perhaps in a similar way as high-Mg andesites in a subduction zone environment (Halla, 2005; Kovalenko et al., 2005). Sanukitoid magmatism is commonly attributed to slab break-off (Halla, 2009; Heilimo et al., 2012), but it is also a possibility that sanukitoids represent melting of metasomatised subcontinental lithospheric mantle during the rebound of a craton after the tectonic activity ceases. Sanukitoid magmatism generally postdates TTG formation, but has so far only been identified in one place in the Archaean craton of Greenland (Steenfelt et al., 2005). An adakitic origin for the GSB andesites can also be ruled out due to the different geochemical characteristics when compared in detail (e.g. Martin, 1999; Martin and Moyen, 2002; Martin et al., 2005).

From recent melt-inclusion studies it has become evident that andesites in modern subduction zone settings are the product of mixing between mafic and felsic magmas in about equal proportions (Kent et al., 2010; Kovalenko et al., 2010; Reubi and Blundy, 2009). Price et al. (2005) argued for a model for modern andesites from New Zealand, where juvenile mafic magmas under-plated the lower crust initiating partial melting of this, and subsequent mixing to produce intermediate compositions. This is much in line with our observations of the geochemical mixing trends for the Grædefjord Supracrustal Belt.

Given that the thermal conditions of the Mesoarchaean were significantly hotter than at present (Herzberg et al., 2010), it would perhaps be possible that large quantities of juvenile mafic magmas that were intruded into the lower portions of hot continental crust, could cause significant melting of the crust and allow for actual magma mixing rather than wall-rock assimilation, exactly as our trace element modelling requires (**Figs. 10 and B19-B22**). Such a scenario is capable of explaining the substantial mixing required by the GSB data. From the compatible trace elements it is evident that

673 an ultramafic third component also interacted with these andesites. This could represent ultramafic
674 picrites, cumulate or mantle rocks.

675 Based on the sum of our new data, we conclude that the Mesoarchaean Grædefjord Supracrustal
676 Belt likely formed in a subduction zone environment. This is consistent with the overall
677 geochemical similarities with modern arc-related andesites. In particular, similar mixing
678 relationships are required for the petrogenesis, of GSB andesites, as those that are observed for
679 andesites in modern subduction zone environments (Kent et al., 2010; Kovalenko et al., 2010;
680 Reubi and Blundy, 2009). This interpretation is consistent with the emerging picture from several
681 distinct lines of evidence for the operation of subduction zone processes since at least the
682 Mesoarchaean (Dhuime et al., 2012; Næraa et al., 2012; Shirey and Richardson, 2011).

683

684 **7. Conclusions**

685

686 • Geochronlogical data from the Tasiusarsuaq terrane suggests the existence of rare remnants
687 of ca. 3200 Ma old continental crust followed by regional volcanism at ca. 2970 Ma, TTG
688 generation at ca. 2900 Ma and metamorphism at ca. 2700 Ma.
689 • We propose the formal name the 'Grædefjord Supracrustal Belt' (GSB) for the ca. 2970 Ma
690 old association of ultramafic to andesitic volcanic rocks, which crop out a few kilometres to
691 the south of Grædefjord, southern West Greenland (**Fig. 1**).
692 • Overall the major and trace element data of the mafic to andesitic rocks of the GSB
693 resembles modern arc-related rocks.
694 • Our trace element modelling reveals that bulk assimilation-fractional-crystallisation (AFC)
695 cannot account for the variations observed in the andesitic leucoamphibolites. Instead the
696 trace element modelling suggests that tholeiitic mafic magmas mixed with 50-80% felsic

magmas of tonalite-trondhjemite-granodiorite (TTG) composition (**Fig. 10**). Although, the exact proportion of the required felsic end-member depends on the actual TTG composition, we would argue that the slightly higher than present mixing ratio is consistent with the hotter Archaean mantle conditions.

- Our Hf and Nd isotope data corroborates a significant crustal contribution in the petrogenesis of the andesitic volcanic rocks in the GSB and are consistent with mixing of about 60% TTG-type crustal-derived melts with juvenile mafic magmas in order to produce the andesitic leucoamphibolites (**Fig. 11**).
- Rare ultramafic rocks in the GSB have enriched trace element patterns (**Fig. 7**), which are similar to picrites reported by Hanski et al. 2001. They have melt-type platinum-group element patterns that are similar to those observed in high-degree mantle melts (**Fig. 8**). We propose that these ultramafic rocks were either derived by melting of metasomatised sub-continental lithospheric mantle or represent arc-related picrites similar to those reported from the Lesser Antilles (Thirlwall et al., 1996).
- The GSB can likely be correlated with the Ikkattup Nunaa Supracrustal Association described by Szilas et al. (2012a) located about 75 km to the south. These two supracrustal belts share many field, geochemical and isotopic features, including clear evidence for significant crustal contamination and mixing in order to explain the geochemical compositions of their andesitic volcanic rocks. Furthermore, both of these supracrustal sequences generally have negative Pb and Sr anomalies, whereas the anorthosites from the Fiskenæsset Complex have large positive Pb and Sr anomalies (Polat et al., 2011b). This together with their similar age and arc-type geochemical features, suggest that this entire region was co-magmatic and that the supracrustal belts represent the shallow volcanic arc-

environment, whereas the Fiskenæsset Complex represents the deeper intrusive and cumulate portion of the same arc complex.

- We propose that modern-style subduction zone processes have been in operation since at least the Mesoarchaean, because of the distinct similarities in the geochemistry of these supracrustal rocks with modern arc rocks, and in particular because of the specific similarities in the petrogenetic mixing model of andesitic rocks as outlined in this study.

Acknowledgements

We acknowledge the Greenland Bureau of Minerals and Petroleum (BMP) for financial support of the field and analytical work, and thank the Geological Survey of Denmark and Greenland (GEUS) for permission to publish this work. We thank Feiko Kalsbeek, Stuart Watt, Agnete Steenfelt and two anonymous reviewers for their constructive comments on an earlier version of the manuscript, which greatly improved this paper. We acknowledge Randall Parrish for the editorial handling of this manuscript. We are grateful for help with the zircon separation at GEUS from Fiorella Fabra Aguilera and Mojagan Alaei. K. Szilas was supported by grant #12-125873 from the Danish Council for Independent Research. J.E. Hoffmann and C. Münker acknowledge support by DFG (German Research Foundation) grants MU 1406/08 and HO 4794/1-1. A. Scherstén acknowledges financial support from the Swedish Research Council through grant #2008-3447. This study is a contribution to IGCP project 599.

References

Bédard, J.H., 2006. A catalytic delamination-driven model for coupled genesis of Archaean crust and sub-continental lithospheric mantle. Geochimica et Cosmochim Acta 70, 1188-1214.

Bézos, A., Lorand, J.P., Humler, E., Gros, M., 2005. Platinum-group element systematics in Mid-Oceanic Ridge basaltic glasses from the Pacific, Atlantic, and Indian Oceans. Geochimica et Cosmochimica Acta 69, 2613-2627.

Bouvier A., Vervoort J.D., Patchett P.J., 2008. The Lu–Hf and Sm–Nd isotopic composition of CHUR: Constraints from unequilibrated chondrites and implications for the bulk composition of terrestrial planets. Earth and Planetary Science Letters 273, 48-57.

Chadwick, B., Coe, K., 1983. Buksefjorden 63 V1 Nord: Descriptive text for geological map of Greenland 1:100,000 - the regional geology of a segment of the Archaean block of southern West Greenland. Grønlands Geologiske Undersøgelse, pp. 70.

Crowley, J.L. 2002. Testing the model of late Archean terrane accretion in southern West Greenland: a comparison of the timing of geological events across the Qarliit nunaat fault, Buksefjorden region. Precambrian Research 116, 57-79.

De Campos, C.P., Perugini, D., Ertel-Ingrisch, W., Dingwell, D.B., Poli, G., 2011. Enhancement of magma mixing effiency by chaotic dynamics: an experimental study. Contribution to Mineralogy and Petrology 161, 863-881.

DePaolo, D.J., 1981. Trace element and isotopic effects of combined wallrock assimilation and fractional crystallization. Earth and Planetary Science Letters 53, 189-202.

Dhuime, B., Hawkesworth, C.J., Cawood, P.A., Storey, C.D., 2012. A change in the geodynamics of continental growth 3 billion years ago. Science 335, 1334-1336.

Ersoy, Y., Helvacı, C., 2010. FC–AFC–FCA and mixing modeler: A Microsoft® Excel© spreadsheet program for modeling geochemical differentiation of magma by crystal fractionation, crustal assimilation and mixing. Computer and Geoscience 36, 383-390.

773 Fiorentini, M.L., Barnes, S.J., Maier, W.D., Brunham, O.M., Heggie, G., 2011. Global variability in the platinum-group
774 element contents of komatiites. Journal of Petrology 52, 83-112.
775
776 Fischer-Gödde, M., Becker, H., Wombacher, F., 2010. Rhodium, gold and other highly siderophile element abundances
777 in chondritic meteorites. Geochimica et Cosmochimica Acta 74, 356-379.
778
779 Friend, C.R.L., Nutman, A.P. McGregor, V.R., 1988. Late Archean terrane accretion in the Godthab region, southern
780 West Greenland. Nature 335, 535-538.
781
782 Friend, C.R.L., Nutman, A.P., 2001. U-Pb zircon study of tectonically bounded blocks of 2940-2840 Ma crust with
783 different metamorphic histories, Paamiut region, South-West Greenland: implications for the tectonic assembly of the
784 North Atlantic craton. Precambrian Research 105, 143-164.
785
786 Garde, A.A., 2007. A mid-Archaean island arc complex in the eastern Akia terrane, Godthåbsfjord, southern West
787 Greenland. Journal of the Geological Society (London) 164, 565-579.
788
789 Georoc database, http://www.georoc.mpch-mainz.gwdg. de/ (accessed May 2013).
790
791 Gerya, T., 2012. Precambrian geodynamics: Concepts and models. Gondwana Research (in press).
792
793 Goldstein, S.B., Francis, D., 2008. The Petrogenesis and Mantle Source of Archaean Ferropicrites from the Western
794 Superior Province, Ontario, Canada. Journal of Petrology 49, 1729-1753.
795
796 Griffin, W.L., Pearson, N.J., Belousova, E., Jackson, S.E., Van Achterbergh, E., O'Reilly, S.Y., Shee, S.R., 2000. The
797 Hf isotope composition of cratonic mantle: LAM-MC-ICPMS analysis of zircon megacrysts in kimberlites. Geochimica
798 et Cosmochimica Acta 64, 133-147.
799
800 Gruau, G., Rosing, M., Bridgwater, D., Gill, R.O.C., 1996. Resetting of Sm-Nd systematics during metamorphism of >
801 3.7-Ga rocks: implications for isotopic models of early Earth differentiation. Chemical Geology 133, 225-240.

Halla, J., 2005. Late Archean high-Mg granitoids (sanukitoids) in the southern Karelian domain, eastern Finland: Pb and Nd isotopic constraints on crust-mantle iteractions. Lithos 79, 161-178.

Halla., J., van Hunen, J., Heilimo, E., Höltta, P., 2009. Geochemical and numerical constraints on Neoarchean plate tectonics. Precambrian Research 174, 155-162.

Hanski, E., Kamenetsky, V.S., 2013. Chrome spinel-hosted melt inclusions in Paleoproterozoic primitive volcanic rocks, northern Finland: Evidence for coexistence and mixing of komatiitic and picritic magmas. Chemical Geology 343, 25-37.

Hanski, E., Huhma, H., Rastas, P., Kamenetsky, V.S., 2001. The Palaeoproterozoic komatiite picrite association of Finnish Lapland. Journal of Petrology 42, 855-876.

Heilimo, E., Halla, J., Andersen, T., Huhma, H., 2012. Neoarchean crustal recycling and mantle metasomatism: Hf-Nd-Pb-O isotope evidence from sanukitoids of the Fennoscandian shield. Precambrian Research 228, 250-266.

Herzberg, C., Condie, K., Korenaga, J., 2010. Thermal history of the Earth and its petrological expression. Earth and Planetary Science Letters 292, 79-88.

Hoffmann, J.E., Münker, C., Næraa, T., Rosing, M.T., Herwartz, D., Garbe-Schönberg, D., Svahnberg, H., 2011. Mechanisms of Archean crust formation inferred from high-precision HFSE systematics in TTGs. Geochimica et Cosmochimica Acta 75, 4157-4178.

Hoffmann, J., Svahnberg, H., Piazolo, S., Scherstén, A., Münker, C., 2012. The geodynamic evolution of Mesoarchean anorthosite complexes inferred from the Naajat Kuuat Complex, southern West Greenland. Precambrian Research 196-197, 149-170.

Kalsbeek, F., Myers, J.S., 1973. The geology of the Fiskenæsset region. Rapport Grønlands Geologiske Undersøgelse 51, 5-18.

Kalsbeek, F., Pidgeon, R.T., 1980. The geological significance of Rb-Sr whole-rock isochrons of polymetamorphic Archaean gneisses, Fiskenaesset area, southern West Greenland. Earth and Planetary Science Letters 50, 225-237.

Kelemen, P.B., Hanghøj, K., Greene, A., 2003. One view of the geochemistry of subduction-related magmatic arcs, with an emphasis on primitive andesite and lower crust. In: Rudnick R.L. (ed.), The Crust, Vol. 3, Treatise on Geochemistry. Holland, H.D., Turekian, K.K., (eds.). Oxford, UK, Elsevier-Pergamon, 593-659.

Kent, A.J., Darr, C., Koleszar, A.M., Salisbury, M.J., Cooper, K.M., 2010. Preferential eruption of andesitic magmas through recharge filtering. Nature Geoscience 3, 631-636.

Kessel, R., Schmidt, M.W., Ulmer, P., Pettke, T., 2005. Trace element signature of subduction-zone fluids, melts and supercritical liquids at 120-180 km depth. Nature 437, 724-727.

Kisters, A.F.M., van Hinsberg, V.J., Szilas, K., 2012. Geology of an Archaean accretionary complex – the structural record of burial and return flow in the Tartoq Group of South West Greenland. Precambrian Research 220-221, 107-122.

Klausen, M.B., Kokfelt, T.F., Keulen, N., Berger, A., Schumacher, J.C., 2011. Geochemistry of Archaean serpentinites, tholeiitic amphibolites and calc-alkaline schists across the Nigerlikasik section in the Kvanefjord Terrane, South-West Greenland, ~62°S. Grønlands Geologiske Undersøgelse Rapport 2011/11.

Klimm, K., Blundy, J.D., Green, T.H., 2008. Trace element partitioning and accessory phase saturation during H_2O-saturated melting of basalt with implications for subduction zone chemical fluxes. Journal of Petrology 49, 523-553.

Kolb, K., Dziggel, A., Koppelberg, M., Stoltz, N.B., Kisters, A.F.M. and Bergen, A. 2010. Controls of hydrothermal quartz vein mineralisation and wall rock alteration between Sermilik and Grædefjord, southern West Greenland. Geological survey of Denmark and Greenland report 2010/47, 73 pp.

Kolb, J., Kokfelt, T.F., Dziggel, A., 2012. Geodynamic setting and deformation history of an Archaean terrane at mid-crustal level: The Tasiusarsuaq terrane of southern West Greenland. Precambrian Research 212-213, 34-56.

Kovalenko, A., Clemens, J.D., Savatenko, V., 2005. Petrogenetic constraints for the genesis of Archaean sanukitoid suites: geochemistry and isotopic evidence from Karelia, Baltic Shield. Lithos 79, 147-160.

Kovalenko, V.I., Naumov, V.B., Girnis, A.V., Dorofeeva, V.A., Yarmolyuk, V.V., 2010. Average composition of basic magmas and mantle sources of island arcs and active continental margins estimated from the data on melt inclusions and quenched rock glasses. Petrology 18, 1-26.

Ludwig, K.R., 2003. Isoplot/Ex 3.00. A geochronological toolkit for Microsoft Excel. Special Publication 4. Berkeley Geochronological Center, Berkeley, CA.

Martin, H., 1999. Adakitic magmas: modern analogues of Archaean granitoids. Lithos 46, 411-429.

Martin, H., Moyen, J.F., 2002. Secular changes in tonalite-trondhjemite-granodiorite composition as markers of the progressive cooling Earth. Geology 30, 319-322.

Martin, H., Smithies, R.H., Rapp, R., Moyen, J.-F., Champion, D., 2005. An overview of adakite, tonalite-trondhjemite-granodiorite (TTG), and sanukitoid: relationships and some implications for crustal evolution. Lithos 79, 1-24.

McGregor, V.R., Friend, C.R.L., 1992. Late Archean prograde amphibolite- to granulite-facies relations in the Fiskenæsset region, southern West Greenland. Journal of Geology 100, 207-219.

Morgavi, D., Perugini, D., De Campos, C.P., Ertl-Ingrisch, W., Lavallée, Morgan, L., Dingwell, D.B., 2012. Interactions between rhyolitic and basaltic melts unraveled by chaotic mixing experiments. Chemical Geology 346, 199-212.

888 Næraa, T., Scherstén, A., 2008. New zircon ages from the Tasiusarsuaq terrane, southern West Greenland. Geological
889 Survey of Denmark and Greenland Bulletin 15, 73-76.
890
891 Næraa T., 2011. Zircon U/Pb, Hf and O isotope systematics from the Archean basement in the Nuùk region, southern
892 West Greenland – Constrains in the early evolution of the continental crust. Ph.D. thesis, University of Copenhagen,
893 Denmark, 195 pp.
894
895 Næraa, T., Scherstén, A., Rosing, M.T., Kemp, A.I.S., Hoffmann, J.E., Kokfelt, T.F., Whitehouse, M.J., 2012. Hafnium
896 isotope evidence for a transition in the dynamics of continental growth 3.2 Gyr ago. Nature 485, 627-630.
897
898 Nutman, A.P., Friend, C.R.L., Baadsgaard, H., McGregor, V.R., 1989. Evolution and assembly of Archean gneiss
899 terranes in the Godthåbsfjord region, southern West Greenland: structural, metamorphic, and isotopic evidence.
900 Tectonics 8, 573-589.
901
902 Nutman, A.P., McGregor, V.R., Friend, C.R.L., Bennett, V C. Kinny, P.D., 1996. The Itsaq Gneiss Complex of
903 southern west Greenland: the world's most extensive record of early crustal evolution (3900–3600 Ma). Precambrian
904 Research 78, 1-39.
905
906 Nutman, A.P. Bennett, V.C. Friend, C.R.L. Horie, K. Hidaka, H., 2007. 3850 Ma tonalites in the Nuuk region,
907 Greenland: geochemistry and their reworking within an Eoarchaean gneiss complex. Contributions to Mineralogy and
908 Petrology 154, 385-408.
909
910 Nutman, A.P., Friend, C.R.L., 2007. Adjacent terranes with ca. 2715 and 2650 Ma high-pressure metamorphic
911 assemblages in the Nuuk region of the North Atlantic Craton, southern West Greenland: Complexities of Neoarchaean
912 collisional orogeny. Precambrian Research 155, 159–203.
913
914 Ohta, T., Arai, H., 2007. Statistical empirical index of chemical weathering in igneous rocks: A new tool for evaluating
915 the degree of weathering. Chemical Geology 240, 280-297.
916

Palme, H., and O'Neill, H.C., 2003. Compositional estimates of mantle composition, in Carlson, R.W., ed., The Mantle and Core, v. 2, Oxford, UK, Elsevier-Pergamon, p. 1-38.

Pearce, J.A., 2008. Geochemical fingerprinting of oceanic basalts with applications to ophiolite classification and the search for Archean oceanic crust. Lithos 100, 14-48.

Perugini, D.,Poli, G., 2012. The mixing of magmas in plutonic and volcanic environments: analogies and differences. Lithos 153, 261-277.

Perugini, D., De Campos, C.P., Ertel-Ingrisch, W., Dingwell, D.B., 2012. The space and time complexity of chaotic mixing of silicate melts: implications for igneous petrology. Lithos 155, 326-340.

Pidgeon, R.T., Kalsbeek, F., 1978. Dating of igneous and metamorphic events in the Fiskenæsset region of southern West Greenland. Canadian Journal of Earth Science 15, 2021-2025.

Polat, A., Kerrich, R., Wyman, D.A., 1998. The late Archean Schreiber-Hemlo and White River-Dayohessarah greenstone belts, Superior Province: collages of oceanic plateaus, oceanic arcs, and subduction-accretion complexes. Tectonophysics 289, 295-326.

Polat, A., R. Kerrich, 2001. Magnesian andesites, Nb-enriched basalt-andesites, and adakites from late-Archean 2.7 Ga Wawa greenstone belts, Superior Province, Canada: implications for late Archean subduction zone petrogenetic processes. Contributions to Mineralogy and Petrology 141, 36-52.

Polat, A., Hofmann, A.W., Rosing, M.T., 2002. Boninite-like volcanic rocks in the 3.7–3.8 Ga Isua greenstone belt, West Greenland: geochemical evidence for intra-oceanic subduction zone processes in the early Earth. Chemical Geology Volume 184, 231-254.

Polat, A., Hofmann, A.W., 2003. Alteration and geochemical patterns in the 3.7-3.8 Ga Isua greenstone belt, West Greenland. Precambrian Research 126, 197–218.

Polat, A., Appel, P.W.U., Frei, R., Pan, Y., Dilek, Y., Ordóñez-Calderón, Fryer, B., Hollis, J.A., Raith, J., 2007. Field and geochemical characteristics of the Mesoarchaean (~3075 Ma) Ivisaartoq greenstone belt, southern West Greenland: evidence for seafloor hydrothermal alteration in supra-subduction zone oceanic crust. Gondwana Research 11, 69–91.

Polat, A., Frei, R., Appel, P.W.U., Dilek, Y., Fryer, B., Ordóñez-Calderón, J.C., Yang, Z., 2008. The origin and compositions of Mesoarchean oceanic crust: Evidence from the 3075 Ma Ivisaartoq greenstone belt, SW Greenland. Lithos 100, 293-321.

Polat, A., Frei, R., Scherstén, A., Appel, P.W.U., 2010. New age (ca. 2970 Ma), mantle source composition and geodynamic constraints on the Archean Fiskenæsset anorthosite complex, SW Greenland. Chemical Geology, 277, 1-20.

Polat, A., Appel, P.W.U., Fryer, B.J., 2011a. An overview of the geochemistry of Eoarchean to Mesoarchean ultramafic to mafic volcanic rocks, SW Greenland: Implication for mantle depletion and petrogenetic processes at subduction zones in the early Earth. Gondwana Research 20, 255-283.

Polat, A., Fryer, B. J., Appel, P. W., Kalvig, P., Kerrich, R., Dilek, Y., Yang, Z., 2011b. Geochemistry of anorthositic differentiated sills in the Archean (~ 2970Ma) Fiskenæsset Complex, SW Greenland: Implications for parental magma compositions, geodynamic setting, and secular heat flow in arcs. Lithos 123, 50-72.

Polat, A., Fryer, B.J., Samson, I.M., Weisener, C., Appel, PW.U., Frei, R., Windley, B., 2012. Geochemistry of ultramafic rocks and hornblendeite veins in the Fiskenæsset layered anorthosite complex, SW Greenland: Evidence for hydrous upper mantle in the Archaean. Precambrian Research 214-215, 124-153.

Rose, N.M., Rosing, M.T., Bridgewater, D., 1996. The origin of metacarbonate rocks in the Isua Archean Supracrustal belt, West Greenland. American Journal of Science 296, 1004-1044.

974 Price, R.C., Gamble, J.A., Smith, I.E.M., Stewart, R.B., Eggins, S., Wright, I.C., 2005. An integrated model for the
975 temporal evolution of andesites and rhyolites and crustal development in New Zealand's North Island. Journal of
976 Volcanology and Geothermal Research 140, 1–24.
977
978 Reubi, O., Blundy, J., 2009. A dearth of intermediate melts at subduction zone volcanoes and the petrogenesis of arc
979 andesites. Nature Letters 461, 1269-1274.
980
981 Riciputi, L.R., Valley, J.W., McGregor, V.R., 1990. Conditions of Archaean granulite metamorphism in the Godthan-
982 Fiskenaesset region, southern West Greenland. Journal of Metamorphic Geology 8, 171-190.
983
984 Rosing, M.T., 1990. The theoretical effect of metasomatism on Sm-Nd isotopic systems. Geochimica et Cosmochimica
985 Acta 54, 1337-1341.
986
987 Savard, D., Barnes, S-J., Meisel, T., 2010. Comparison between Ni-fire assay Te-copercipitation and isotope dilution
988 with high pressure asher acid digestion for the determination of platinum-group elements, rhenium and gold.
989 Geostandards and Geoanalytical Research 34, 281-291.
990
991 Schumacher, J.C., van Hinsberg, V.J., Keulen, N., 2011. Metamorphism in supracrustal and ultramafic rocks in
992 southern West Greenland 64-61.5°N. Danmarks og Grønlands Geologiske Undersøgelse Rapport 2011/6, 30 pp.
993
994 Shirey, S.B., Richardson, S.H., 2011. Start of the Wilson cycle at 3 Ga shown by diamonds from subcontinental mantle.
995 Science 333, 434-436.
996
997 Skulski, T., Percival, J.A., 1996. Allochthonous 2.78 Ga oceanic plateau slivers in a 2.72 Ga continental arc sequence:
998 Vizien greenstone belt, northeastern Superior Province, Canada. Lithos 37, 163-179.
999
1000 Souders, A.K., Sylvester, P.J., Myers., J.S., 2012. Mantle and crustal sources of Archean anorthosite: a combined in situ
1001 isotopic study of Pb–Pb in plagioclase and Lu–Hf in zircon. Contributions to Mineralogy and Petrology 165, 1-24.
1002

Stern, R.A., Hanson, G.N., Shirey, S.B., 1989. Petrogenesis of mantle-derived LILE-enriched Archean monzodiorites and trachyandesites (sanukitoids) in southwestern Superior. Canadian Journal of Earth Sciences 26, 1688-1712.

Szilas, K., Hoffmann, J.E., Scherstén, A., Rosing, M.T., Kokfelt, T.F., Windley, B.F., van Hinsberg, V.J., Næraa, T., Keulen, N., Frei, R., Münker, C., 2012a. Complex calc-alkaline volcanism recorded in Mesoarchaean supracrustal belts north of Frederikshåb Isblink, southern West Greenland: implications for subduction zone processes in the early Earth. Precambrian Research, 208-211, 90-123.

Szilas, K., Scherstén, A., Næraa, T., Stendal, H., Rosing, M.T., Kokfelt, T.F., V.J., Frei, R., 2012b. Origin of Mesoarchaean arc related rocks with boninite/komatiite affinities from southern West Greenland. Lithos, 144-145, 24-39.

Szilas, K., Van Hinsberg, J., Kisters, A.F.M., Hoffmann, E.J., Kokfelt, T.F., Scherstén, A., Windley, B.F., Frei, R., Rosing, M.T., Münker, C., 2013. Remnants of Mesoarchean suprasubduction zone oceanic crust in the Tartoq Group, SW Greenland. Gondwana Research 23, 436-451.Szilas, K., Garde, A.A. Mesoarchaean aluminous rocks at Storø, southern West Greenland: new age data and evidence of premetamorphic seafloor weathering of basalts. Chemical Geology (in press).

Thirlwall, M. F., Graham, A. M., Arculus, R. J., Harmon, R. S., Macpherson, C. G., 1996. Resolution of the effects of crustal assimilation, sediment subduction, and fluid transport in island arc magmas: Pb-Sr-Nd-O isotope geochemistry of Grenada, Lesser Antilles. Geochimica et Cosmochimica Acta 60, 4785-4810.

Thompson, P.M.E., Kempton, P.D., Kerr, A.C., 2008. Evaluation of the effects of alteration and leaching on Sm-Nd and Lu-Hf systematics in submarine mafic rocks. Lithos 104, 164-176.

Van Gool, J.A.M., Scherstén, A., Østergaard, C., Neraa, T., 2007. Geological setting of the Storø gold prospect, Godhåbsfjord region, southern West Greenland. Danmarks og Grønlands Geologiske Undersøgelse Rapport 2007/83, 150 pp.

1032 Van Kranendonk, M.J., 2011. Onset of Plate Tectonics. Science, 333, 413-414.
1033
1034 Weiss, Y., Griffin, W.L., Bell, D.R., Navon, O., 2011. High-Mg carbonatitic melts in diamonds, kimberlites and the
1035 sub-continental lithosphere. Earth and Planetary Science Letters 309, 337-347.
1036
1037 Wilf, C.I.Z. 1982. Geokemien af de grå amphiboliter, en del af en supracrustal bjergartsenhed, ved Grædefjorden, nord
1038 for bygden Qeqertarsuatsiaat (Fiskenæsset) i den centrale del af Sydvestgrønland. Unpublished M.Sc. thesis, Aarhus
1039 University, 145 pp.
1040
1041 Windley, B., Garde, A.A., 2009. Arc-generated blocks with sections in the North Atlantic craton of West Greenland:
1042 Crustal growth in the Archean with modern analogues. Earth-Science Reviews 93, 1-30.
1043
1044 Wittig, N., Pearson, D.G., Webb, M., Ottley, C. J., Irvine, G. J., Kopylova, M., Jensen, S.M., Nowell, G. M., 2008.
1045 Origin of cratonic lithospheric mantle roots: A geochemical study of peridotites from the North Atlantic Craton, West
1046 Greenland. Earth and Planetary Science Letters 274, 24-33.
1047
1048 Woodland, S.J., Pearson, D.G., Thirlwall, M.F., 2002. A platinum group element and Re-Os isotope investigation of
1049 siderophile element recycling in subduction zones: comparison of Grenada, Lesser Antilles Arc, and the Izu-Bonin Arc.
1050 Journal of Petrology 43, 171-198.
1051

1052 **Figure captions**

1053

1054 Figure 1. Geological map of SW Greenland showing the major crustal lithological units. The
1055 location of the Grædefjord Supracrustal Belt is outlined by the red box. Based on mapping by
1056 GEUS.

1057

1058 Figure 2. Field photos showing examples of possible magmatic structures. a) Mafic dyke with
1059 quartz-plagioclase macrocrysts in dark amphibolite groundmass (pencil for scale). b)

Leucoamphibolite with large felsic fragments which could represent ‘bombs’ and ‘lapilli’ (hammer is about 1 m). c) Layered leucoamphibolite with distinct modal variation (pencil for scale). d) Leucoamphibolite with felsic patches that may have been relict volcaniclastic fragments.

Figure 3. Variation diagrams for major elements versus MgO. Note that the leucoamphibolites generally form an array with the TTGs and the mafic rocks as end-members.

Figure 4. Variation diagrams for trace elements versus MgO. Note that the leucoamphibolites generally also form an array with the TTGs and the mafic rocks as end-members, but certain compatible elements form arrays between the TTGs and the ultramafic rocks.

Figure 5. Primitive mantle-normalised (Palme and O’Neill, 2003) trace element diagrams for the amphibolites, mafic dykes, leucoamphibolites and the TTGs.

Figure 6. The discrimination diagram of Pearce (2008) with all lithological units from the Grædefjord Supracrustal Belt plotted. The samples generally plot above the mantle array and within the arc-related field, except for on amphibolite (sample 508219) and the ultramafic rocks.

Figure 7. Primitive mantle-normalised (Palme and O’Neill, 2003) trace element diagrams for the ultramafic rocks. Note the fractionated HREE pattern, which suggest garnet was present in the source of these rocks.

Figure 8. Platinum-group element patterns for the ultramafic rocks normalised to chondrite (Fischer-Gödde et al., 2010). For comparison we have measured ultramafic cumulate rocks from the

Ikkattup Nunaa Supracrustal Association (INSA) and also show the median patterns for three different types of komatiites (data from Fiorentini et al., 2011).

Figure 9. εHf_t evolution of the Grædefjord Supracrustal rocks since 2970 Ma as a function of time. DM from Griffen et al. (2000) and CHUR values of Bouvier et al. (2008).

Figure 10. Y vs. Ti diagram for the Grædefjord Supracrustal Belt. Our AFC model cannot account for the observed variation in the leucoamphibolites, whereas a simple binary mixing model provides a much better fit. See **Figures B19-B22** in the online supplementary **Appendix B** for more examples of our trace element modelling.

Figure 11. $^{176}Hf/^{177}Hf$ vs. time diagram showing the isotopic constraints for the mixing process. As the contaminant we use sample 468645 from Næraa et al. (2012), which is a TTG gneiss of appropriate age (3255 Ma) from the Tasiusarsuaq terrane. The Grædefjord amphibolites and mafic dykes can be explained by about 25% mixing with older TTG-type crust. About 60% mixing of felsic crust with 40% juvenile mafic magma (sample 511116) can explain the observed isotopic shift in the leucoamphibolites. Alternatively the leucoamphibolites were in fact derived from source with a chondritic isotope composition. DM from Griffen et al. (2000) and CHUR values of Bouvier et al. (2008).

Figure captions for Inline figures

Figure B15. LA-ICP-MS zircon U-Pb isotope data for felsic intrusive rocks. a) Probability density diagram (PDD) for the crosscutting TTG sheet (sample 511110). b) Concordia diagram for TTG

sheet (511110) indicating an age of 2888 ±6.8 Ma. c) PDD for the plagioclase-rimmed magnetite phenocrysts-bearing TTG sheet (sample 508221). d) Concordia diagram for sample 508221 with an age of 2708 ±11 Ma. e) PDD for a pegmatite sheet (sample 511134). f) Concordia diagram for the pegmatite suggesting a main event at 2731 ±19 Ma.

Figure B16. LA-ICP-MS zircon U-Pb isotope data for the leucoamphibolites. Left-hand column show PDDs centred on ca. 2720 Ma and the right-hand column shows concordia diagrams for the corresponding peaks after filtering (see Section 5.3 for details).

Figure B17. LA-ICP-MS zircon U-Pb isotope data for the mafic dyke sample 508218 with an age population centred on 2717.5 ±7.6 Ma.

Figure B23. Lu-Hf isochron diagram with samples from Szilas et al. (2012) in blue and four mafic samples from the Grædefjord Supracrustal Belt in red.

Online Supplementary Material

Appendix A - Analytical methods descriptions.

Appendix B - Supplementary geochemical diagrams.

Table 1 - Whole-rock major and trace element data.

Table 2 - Platinum group element data.

1132

1133 Table 3 - Whole-rock Sm-Nd and Lu-Hf isotope data.

1134

1135 Table 4 - Zircon U-Pb isotope data.

Appendix A - Analytical methods descriptions.

Appendix B - Supplementary geochemical diagrams.

Table 1 – Whole-rock major and trace element data.

Table 2 - Platinum group element data.

Table 3 – Whole-rock Sm-Nd and Lu-Hf isotope data.

Table 4 - Zircon U-Pb isotope data.

Figure 1

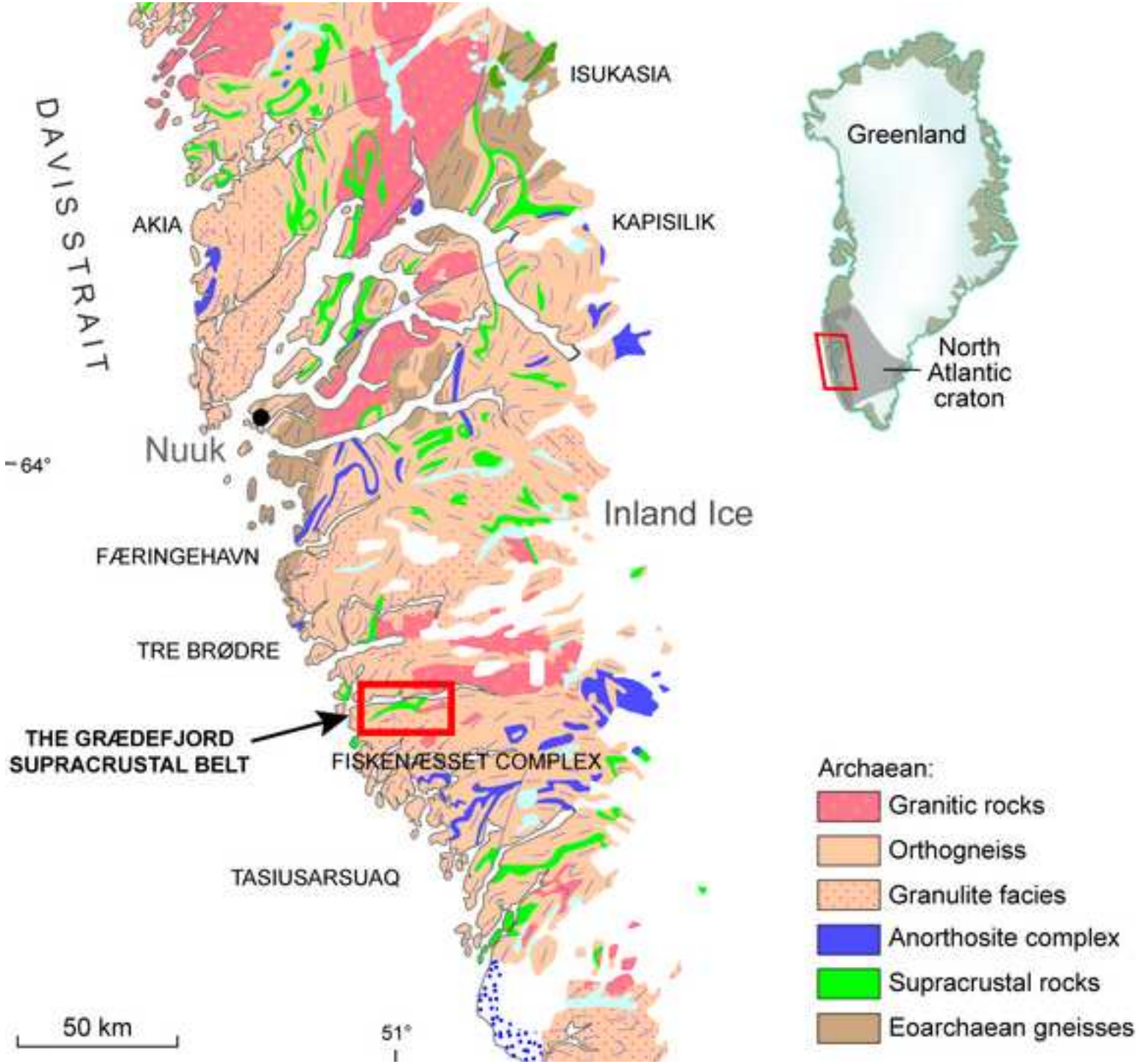
ISUKASIA
DAVIS STRAIT
AKIA
KAPISILIK
Nuuk
64°
Inland Ice
FÆRINGEHAVN
TRE BRØDRE
THE GRÆDEFJORD
SUPRACRUSTAL BELT
FISKENÆSSET COMPLEX
TASIUSARSUAQ
50 km
51°
Greenland
North
Atlantic
craton
Archaean:
Granitic rocks
Orthogneiss
Granulite facies
Anorthosite complex
Supracrustal rocks
Eoarchaean gneisses

Figure 2

Figure 3

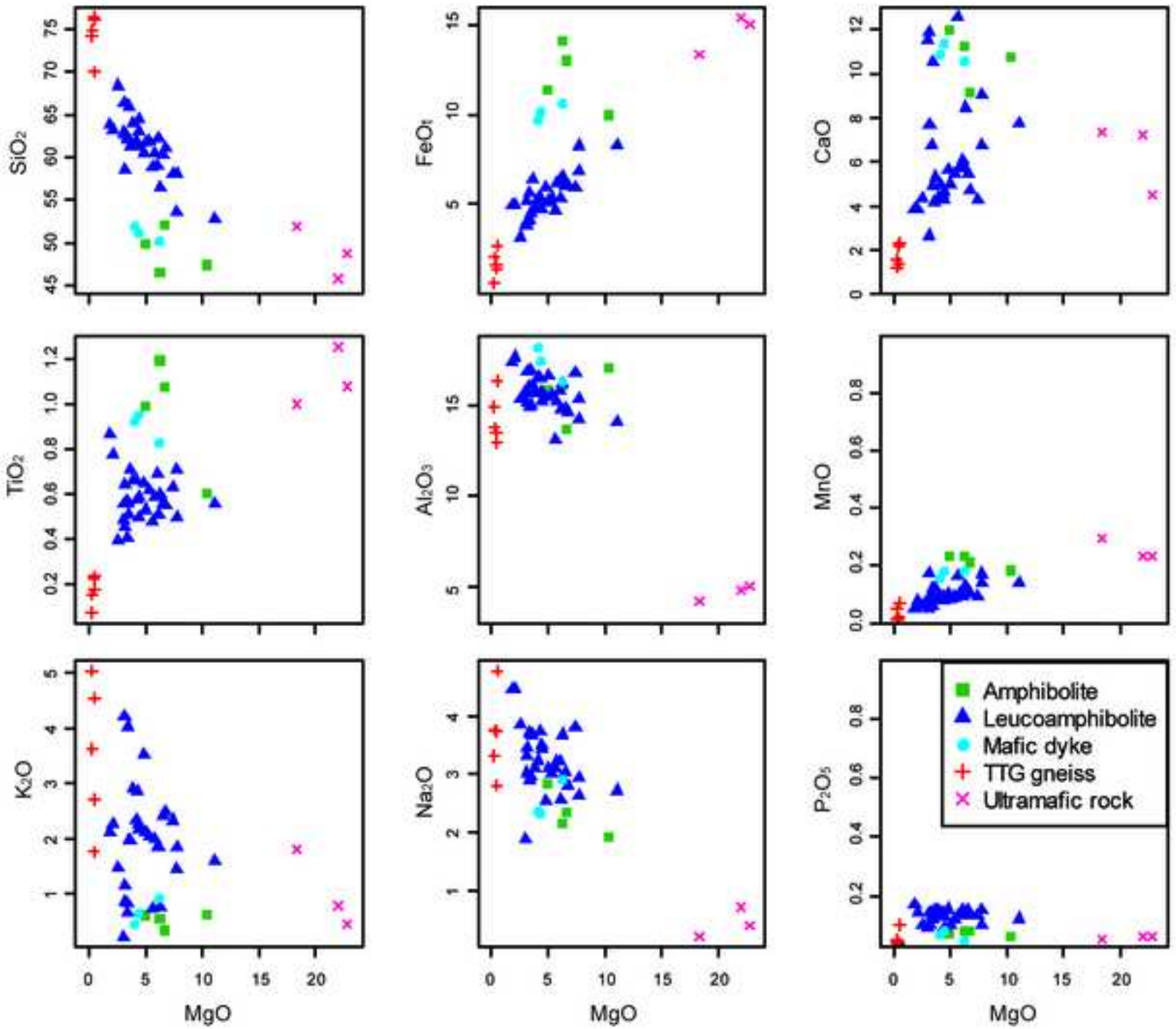
SiO2
FeOt
CaO
TiO2
Al2O3
MnO
K2O
Na2O
P2O5
MgO
MgO
MgO
Amphibolite
Leucoamphibolite
Mafic dyke
TTG gneiss
Ultramafic rock

Figure 4

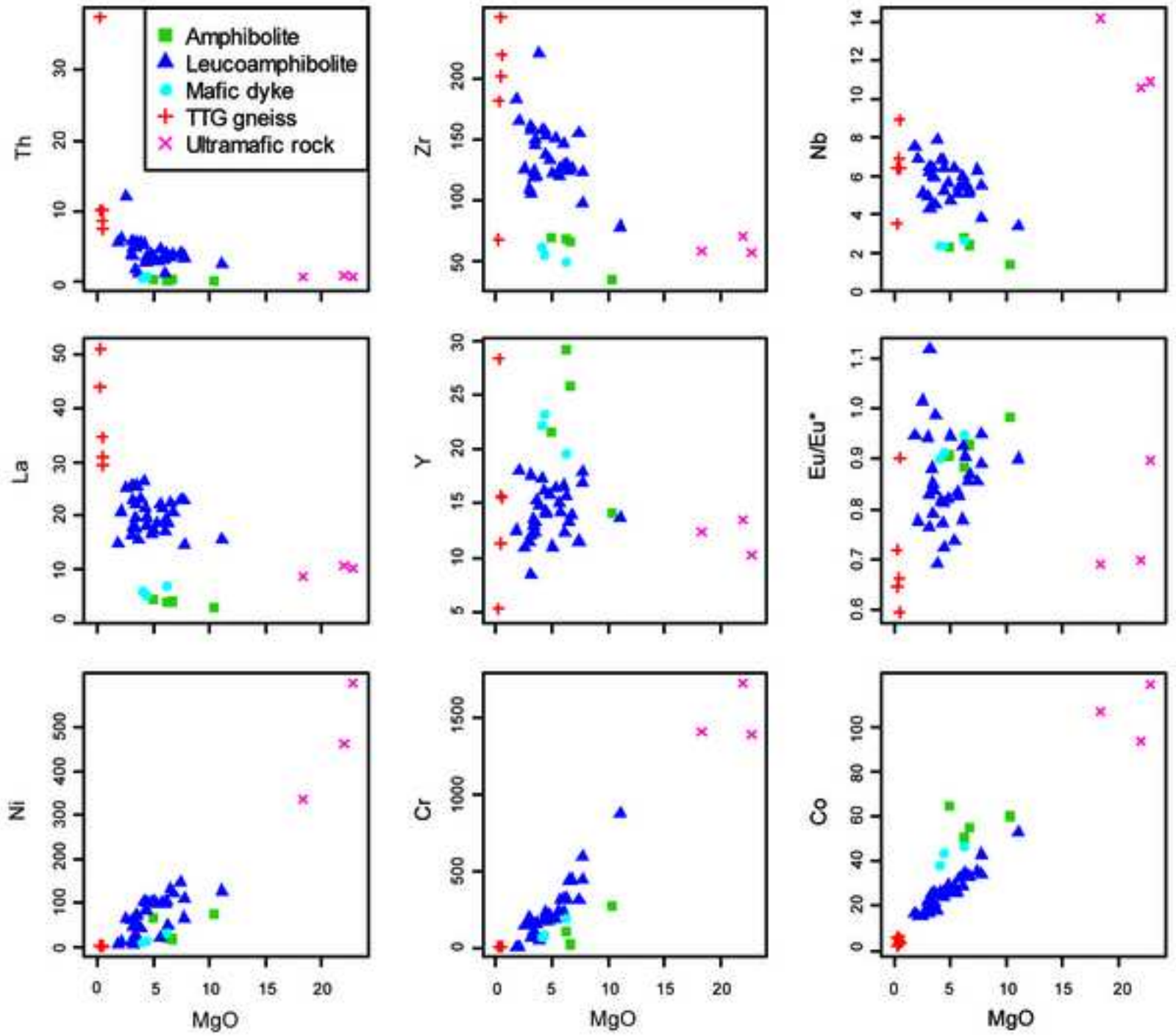
Amphibolite
Leucoamphibolite
Mafic dyke
TTG gneiss
Ultramafic rock
Th
Zr
Nb
La
Y
Eu/Eu*
Ni
Cr
Co
MgO
MgO
MgO

Figure 5

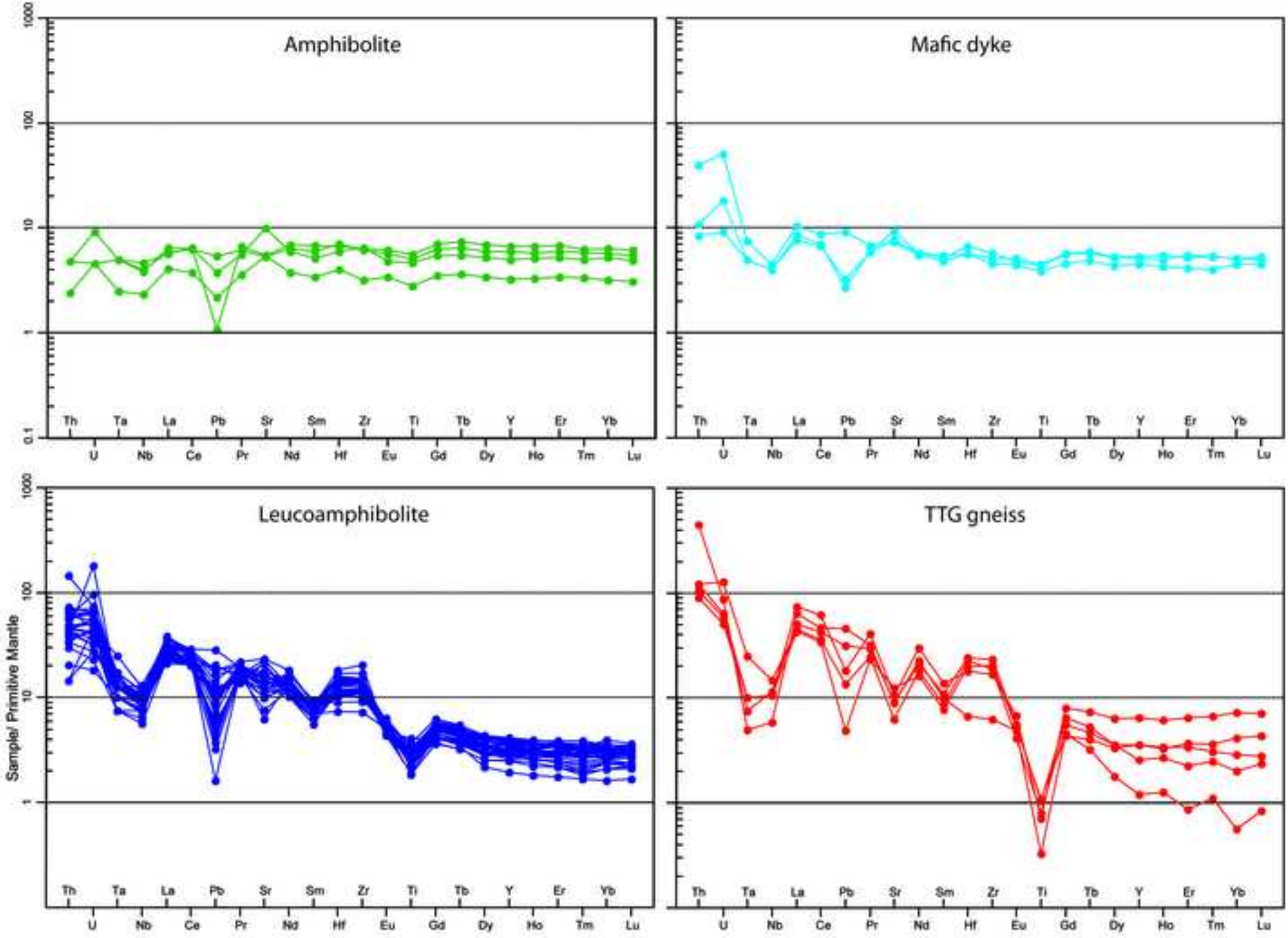
Amphibolite
Mafic dyke
Leucoamphibolite
TTG gneiss
Sample/ Primitive Mantle
1000
100
10
1
0.1
Th Ta La Pb Sr Sm Zr Ti Tb Y Er Yb
U Nb Ce Pr Nd Hf Eu Gd Dy Ho Tm Lu

Figure 6

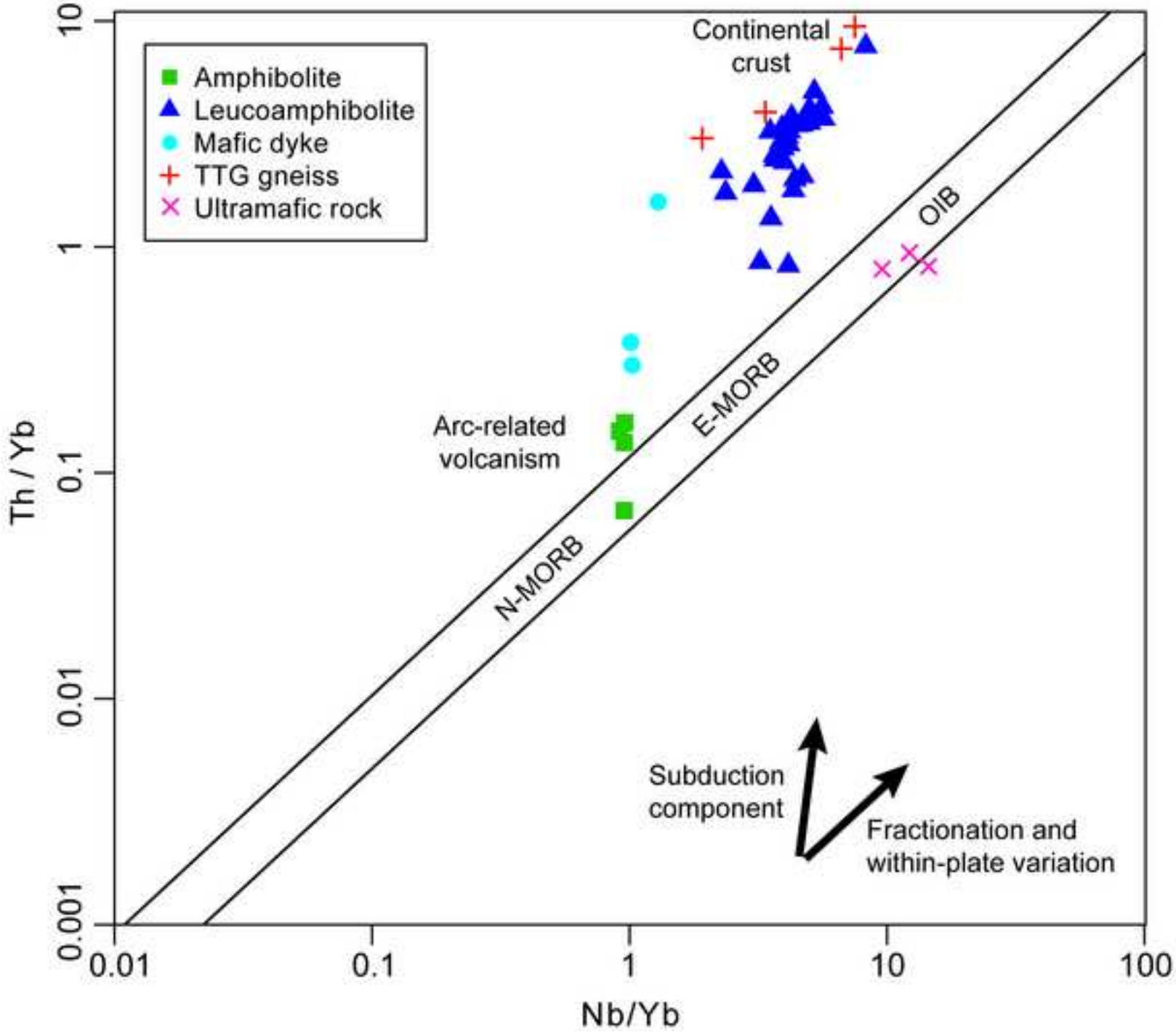
Amphibolite
Leucoamphibolite
Mafic dyke
TTG gneiss
Ultramafic rock
Continental crust
Arc-related volcanism
N-MORB
E-MORB
OIB
Subduction component
Fractionation and within-plate variation
Th / Yb
Nb/Yb
10
1
0.1
0.01
0.001
0.01
0.1
1
10
100

Figure 7

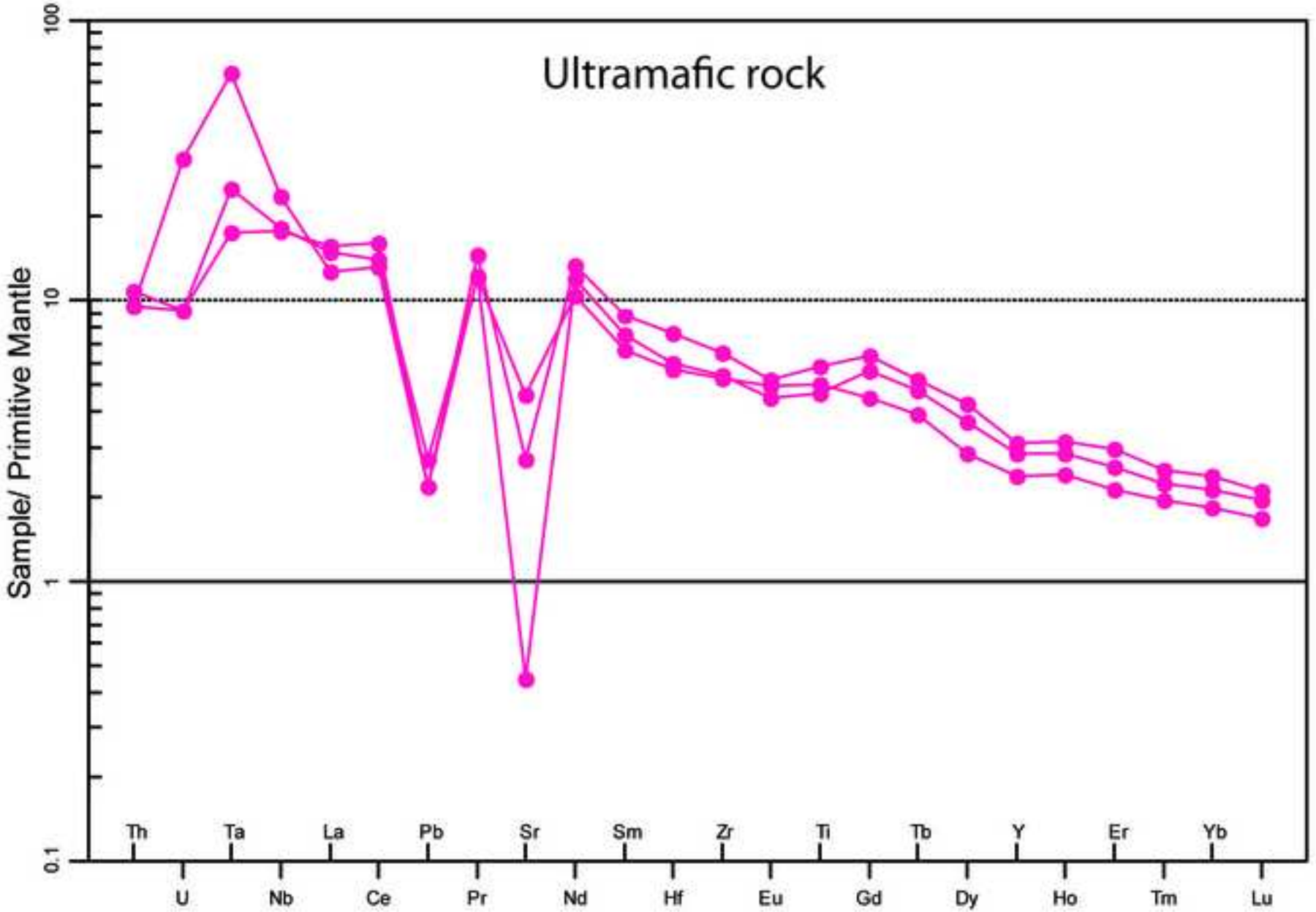
Ultramafic rock
Sample/ Primitive Mantle
100
10
1
0.1
Th
U
Ta
Nb
La
Ce
Pb
Pr
Sr
Nd
Sm
Hf
Zr
Eu
Ti
Gd
Tb
Dy
Y
Ho
Er
Tm
Yb
Lu

Figure 8

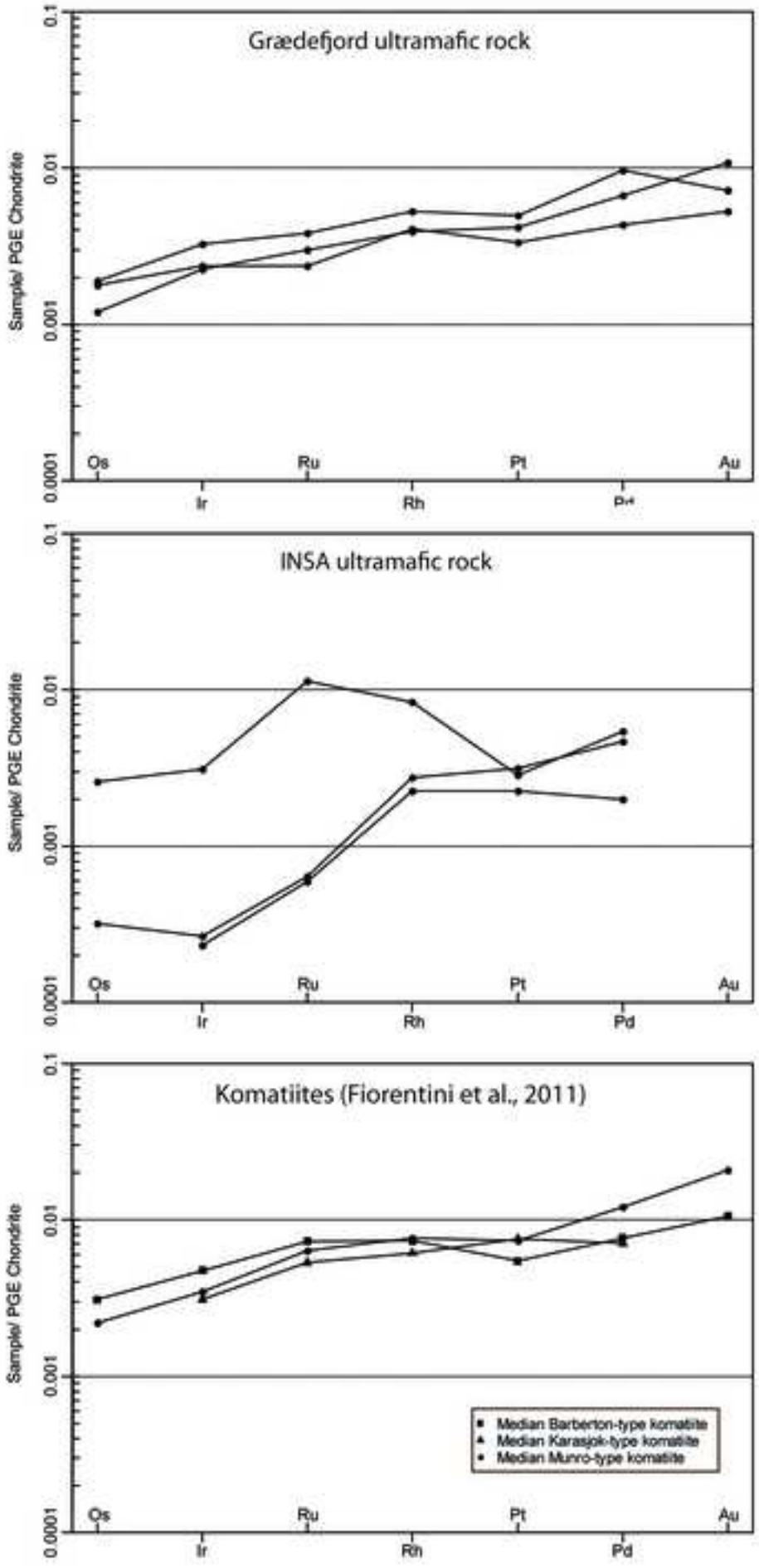
Grædefjord ultramafic rock
INSA ultramafic rock
Komatiites (Fiorentini et al., 2011)
Sample/ PGE Chondrite
0.1
0.01
0.001
0.0001
Os
Ir
Ru
Rh
Pt
Pd
Au
Median Barberton-type komatiite
Median Karasjok-type komatiite
Median Munro-type komatiite

Figure 9

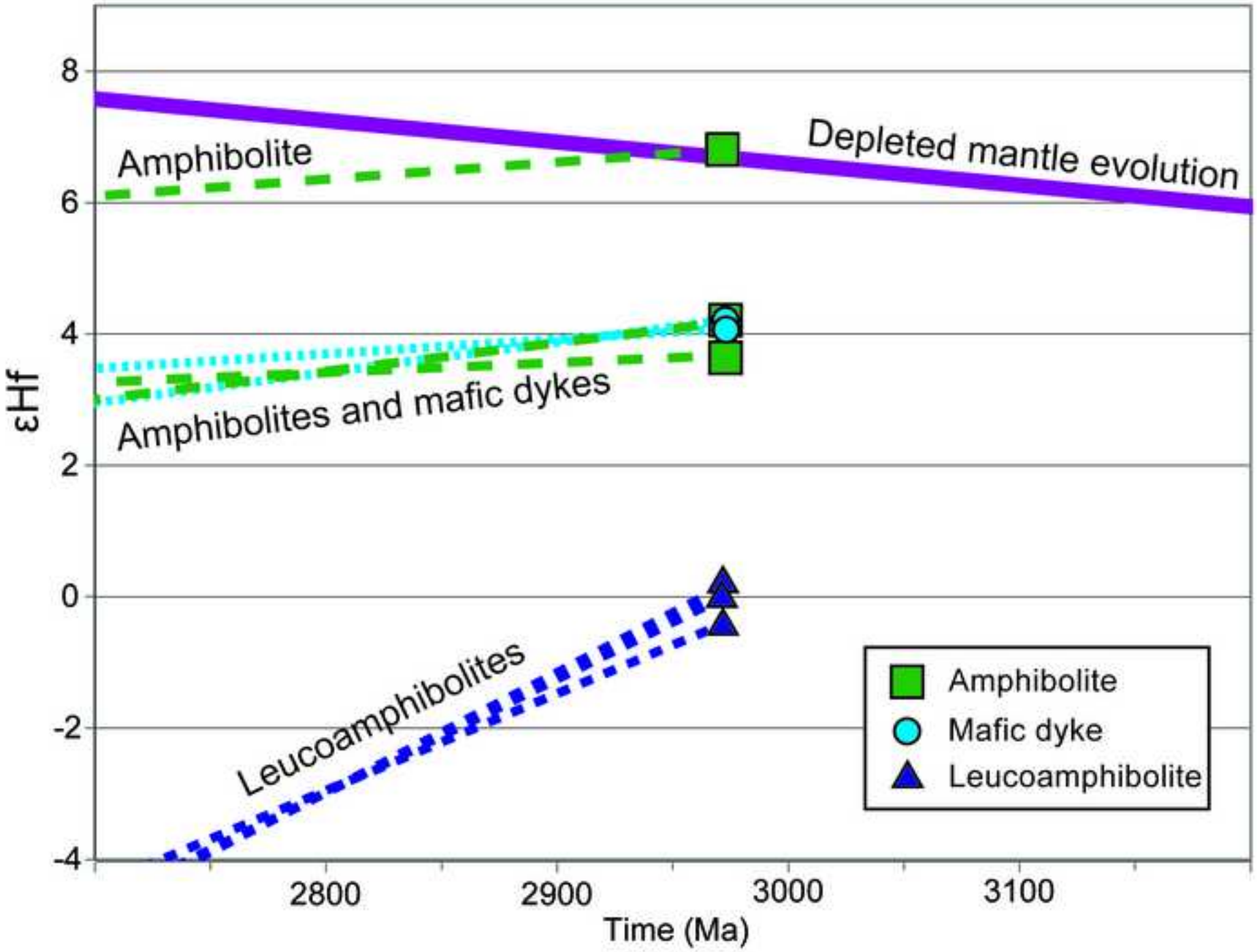
8
6
4
2
0
-2
-4
εHf
2800
2900
3000
3100
Time (Ma)
Depleted mantle evolution
Amphibolite
Amphibolites and mafic dykes
Leucoamphibolites
Amphibolite
Mafic dyke
Leucoamphibolite

Figure 10

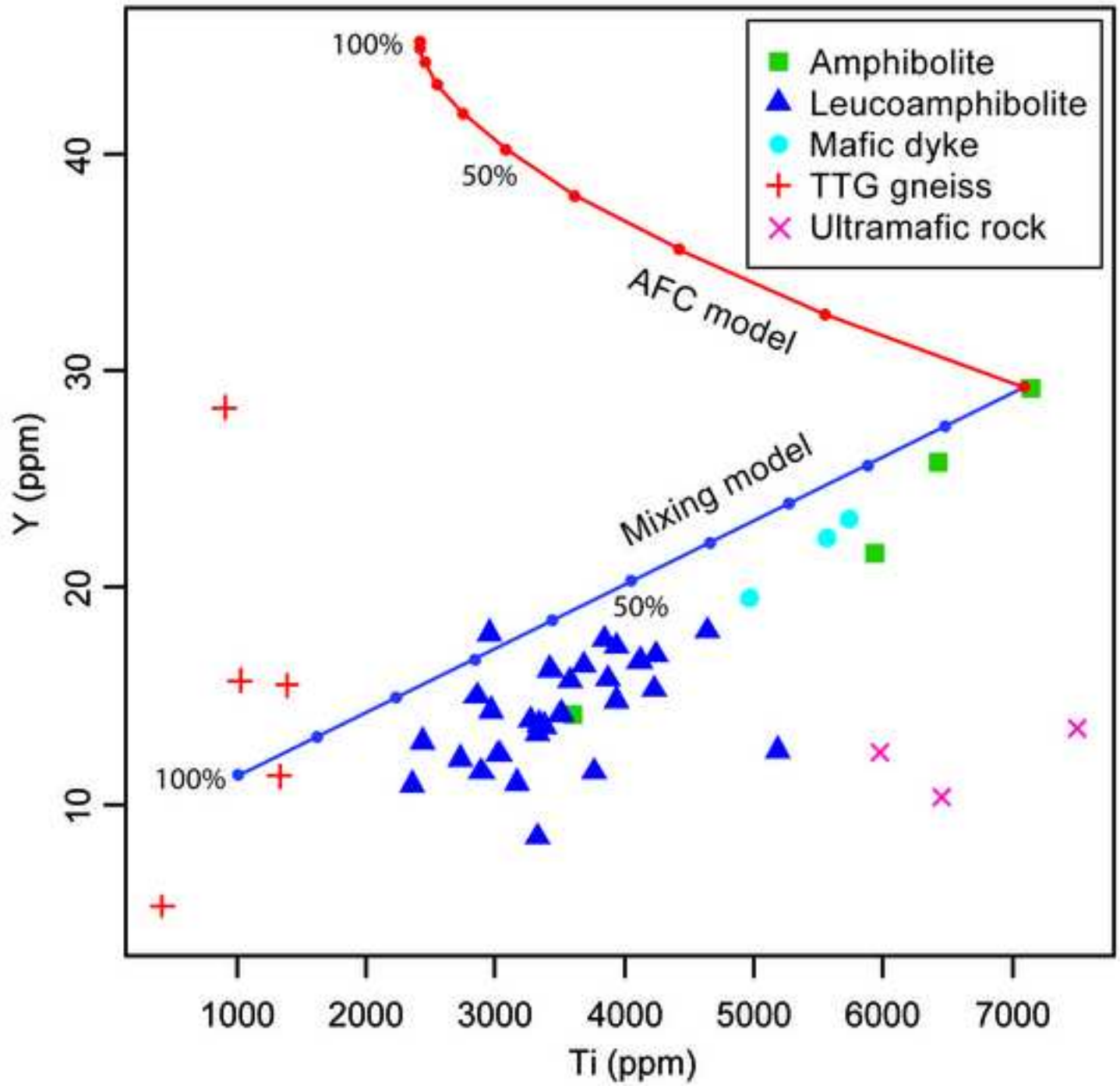
100%
50%
AFC model
Mixing model
50%
100%
Amphibolite
Leucoamphibolite
Mafic dyke
TTG gneiss
Ultramafic rock
Y (ppm)
10
20
30
40
1000
2000
3000
4000
5000
6000
7000
Ti (ppm)

Figure 11

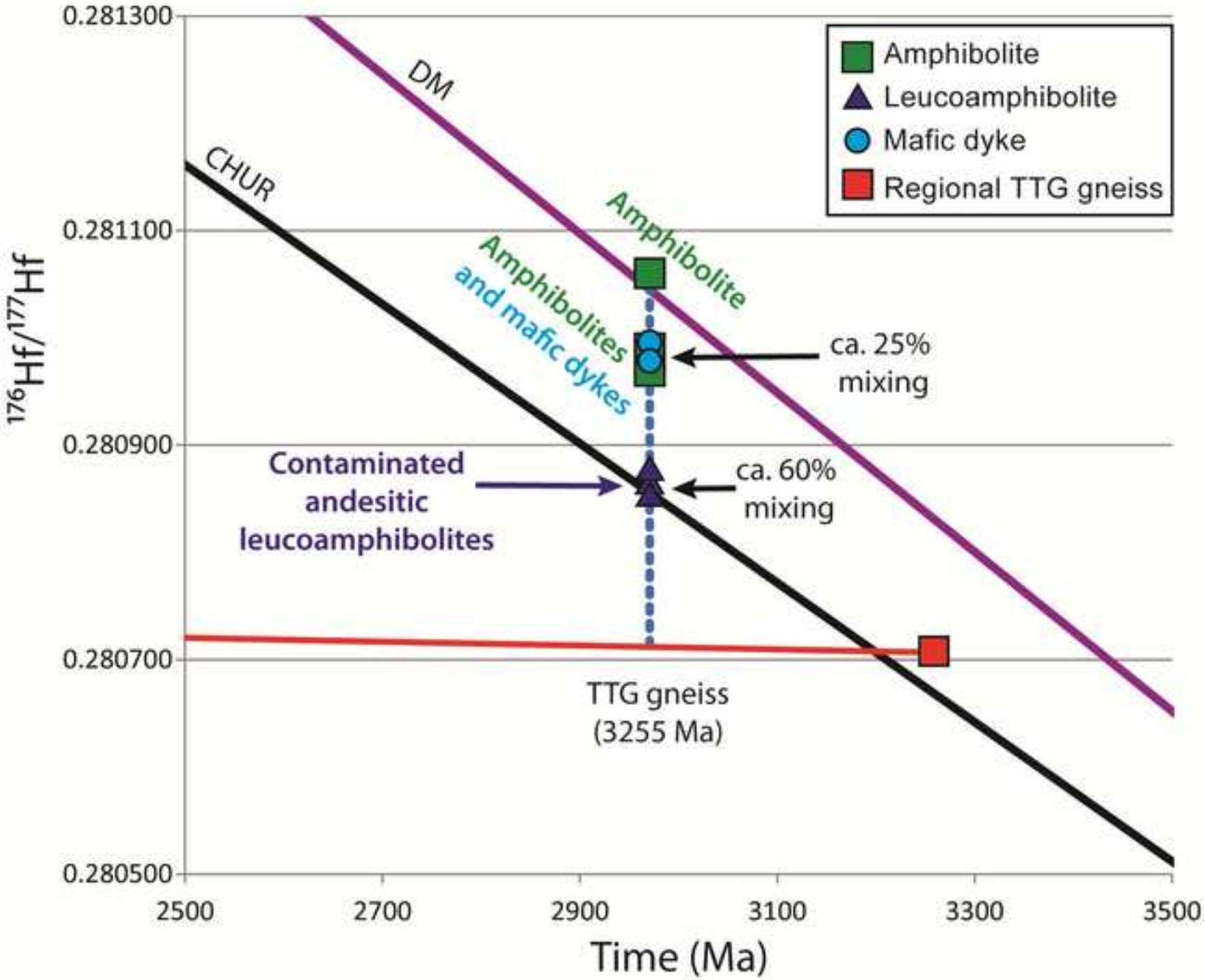
0.281300
0.281100
0.280900
0.280700
0.280500
$^{176}Hf/^{177}Hf$
2500
2700
2900
3100
3300
3500
Time (Ma)
DM
CHUR
Amphibolite
Amphibolites and mafic dykes
ca. 25% mixing
Contaminated andesitic leucoamphibolites
ca. 60% mixing
TTG gneiss (3255 Ma)
Amphibolite
Leucoamphibolite
Mafic dyke
Regional TTG gneiss

Inline Supplementary Figure

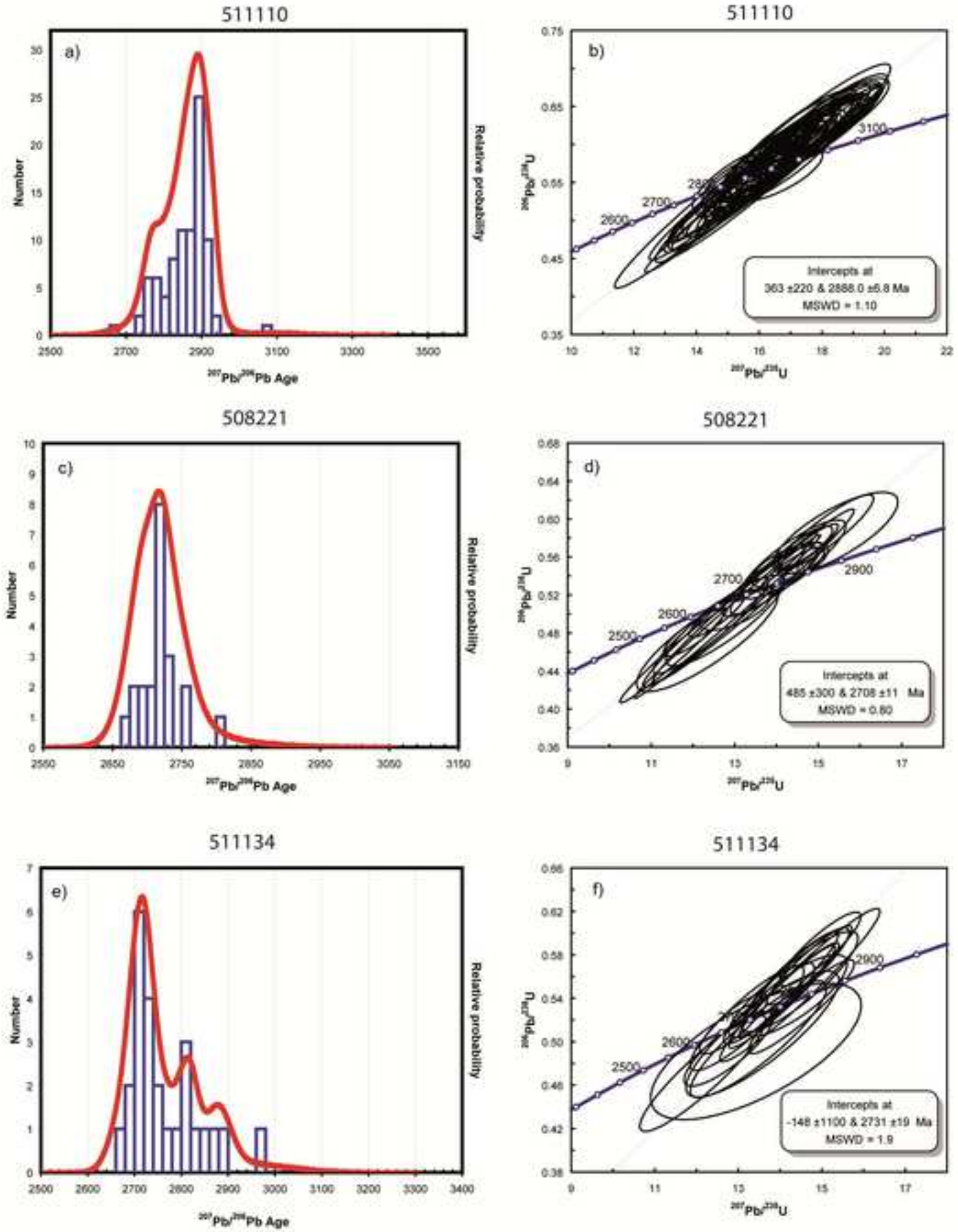

Inline Supplementary Figure

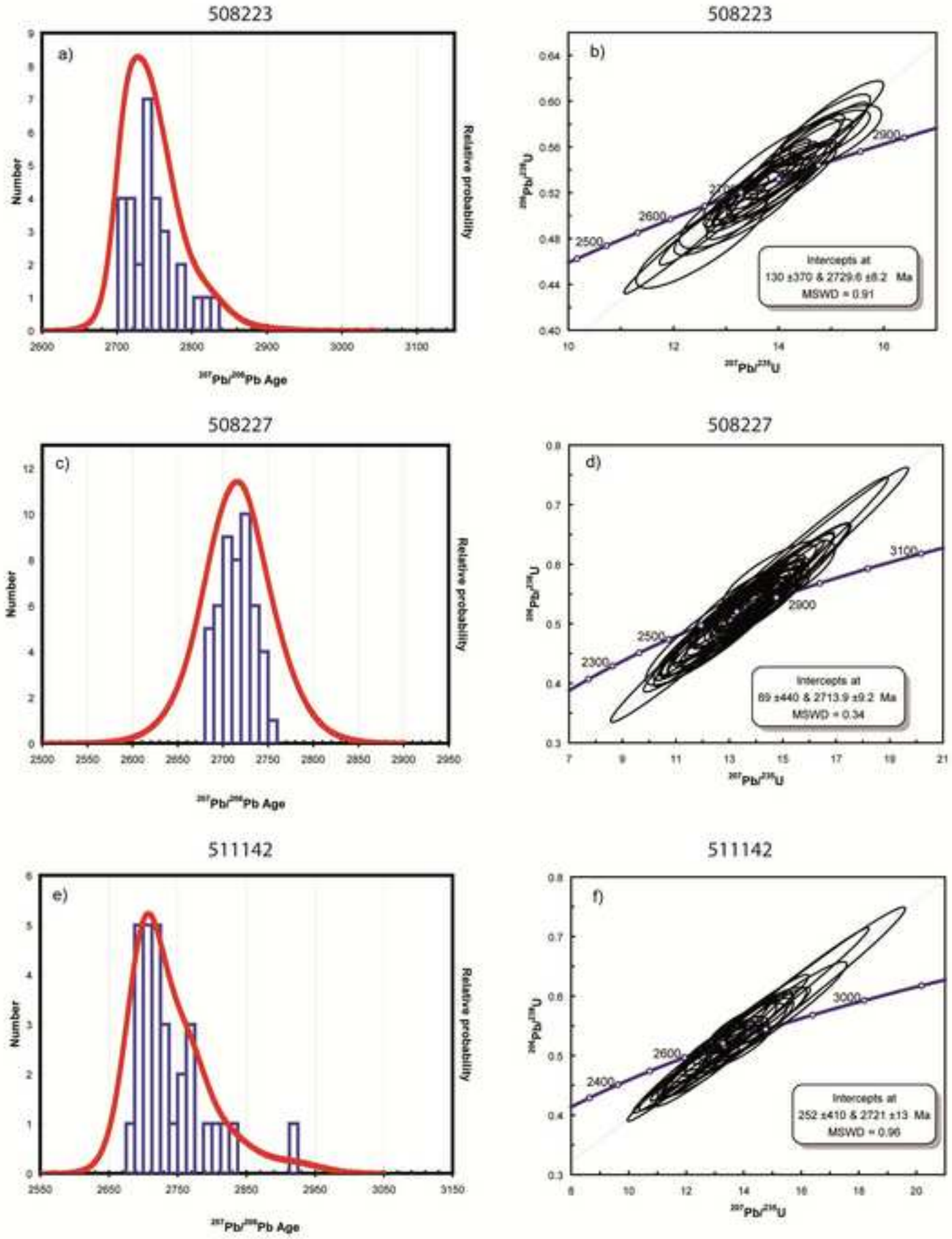

Inline Supplementary Figure

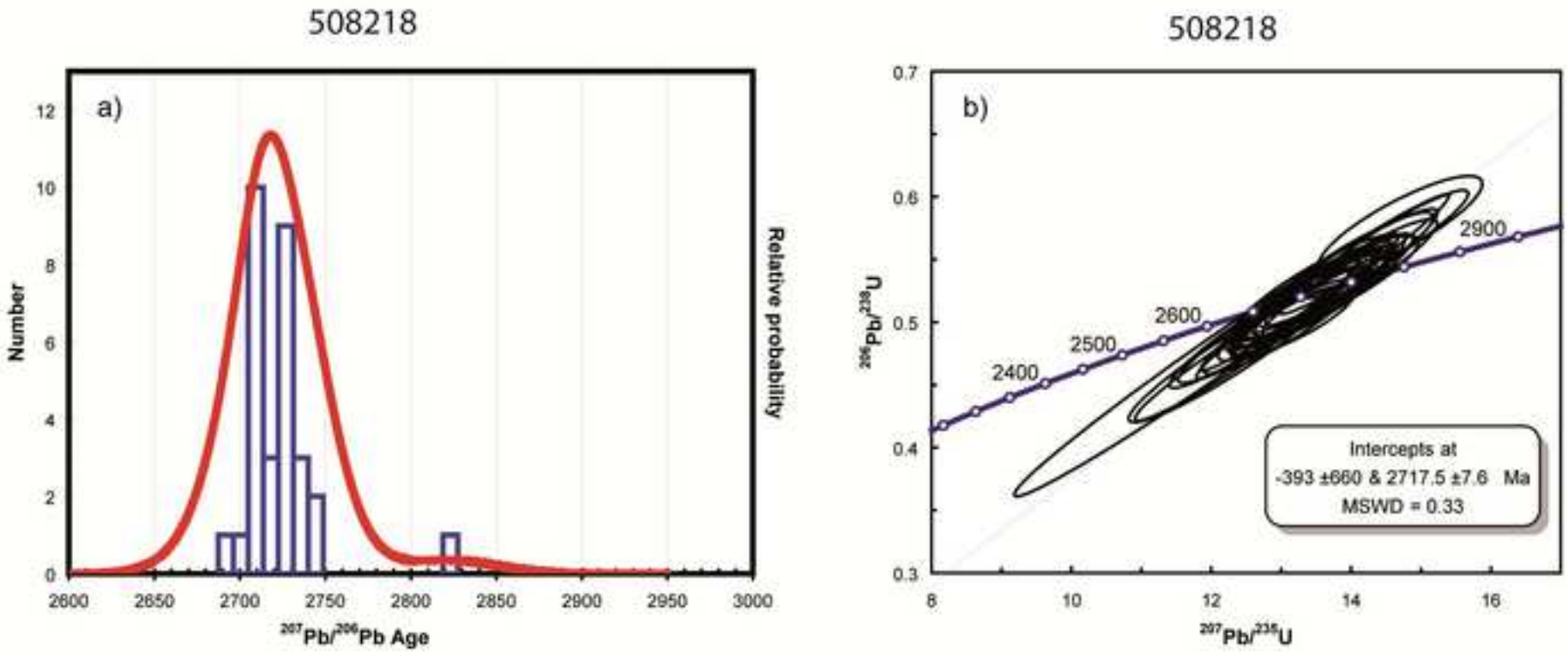

Inline Supplementary Figure